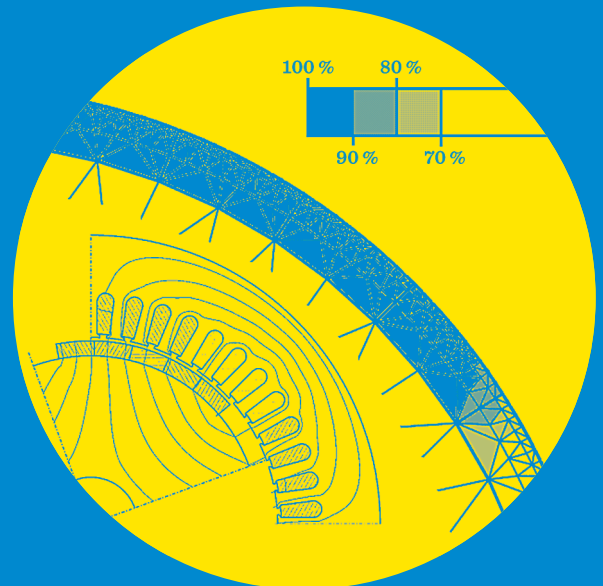**Department of Electrical Engineering**

Modeling Demagnetization of Sintered NdFeB Magnet Material in Time-Discretized Finite Element Analysis

Sami Ruoho

Modeling Demagnetization of Sintered NdFeB Magnet Material in Time-Discretized Finite Element Analysis

Sami Ruoho

Doctoral dissertation for the degree of Doctor of Science in Technology to be presented with due permission of the Faculty of Electronics, Communications and Automation for public examination and debate in Auditorium S4 at the Aalto University School of Electrical Engineering (Espoo, Finland) on the 14th of January 2011 at 12 noon.

Aalto University
School of Electrical Engineering
Department of Electrical Engineering

Abstract

The aim of this work was to develop a tool able to simulate the behavior of a permanent magnet machine after demagnetization. The tool would include a demagnetization model, an eddy current model, and a thermal model. The eddy current calculation accuracy in two-dimensional geometries will also be improved. The other goals were to study how the demagnetization should be modeled in different situations and to evaluate a mixed-grade pole idea, where there can be several magnet grades in a pole of a machine.

A demagnetization model based on an exponential function was developed. The new model can be defined by using only four parameters. The new model can take into account the squareness of the hysteresis curve. The new model also takes into account the demagnetizing field perpendicular to the orientation direction, which is often ignored. The demagnetization model was implemented in an existing finite element method model. The demagnetization model was evaluated by modeling a locked-rotor situation of a permanent magnet machine. The simulation results were compared with the demagnetization of the magnets of a real motor after the same situation. It was discovered that the demagnetization model can accurately predict the demagnetization of the magnets in a permanent magnet machine.

The resistivity of NdFeB permanent magnet material was measured as a function of temperature. The resistivity of rare earth magnet materials was found to be anisotropic. It was shown that the resistivity can be treated as an isotropic scalar property, as long as the resistivity value perpendicular to the magnetization direction of the magnets is used.

An eddy current model was developed. The eddy current model modifies the resistivity of the magnet material as a function of temperature and as a function of the shape of the magnet. The modification as a function of the shape was shown to improve the accuracy of the eddy current calculation in two-dimensional modeling.

The modeling of the demagnetization was studied with simulations using an overheated motor loaded with a constant torque as an example. It was shown that it is important to include a thermal model in the demagnetization calculations.

The mixed-grade pole machine was used as a calculation example in the simulations. It was shown that a slight improvement in the performance of the machine can be achieved with a simultaneous potential for cost savings by using a mixed-grade pole.

Tiivistelmäteksti

Työn tavoitteena oli kehittää työkalu, jolla voidaan mallintaa kestomagneettikoneen suorituskyky sen jälkeen, kun koneen kestomagneetit ovat demagnetoituneet osittain. Työkalu koostuu demagnetoitumis-, lämpö- ja pyörrevirtamallista. Tavoitteena oli myös kaksiulotteisen pyörrevirtalaskennan tarkkuuden parantaminen. Muina tavoitteina oli tarkastella, miten demagnetointimallinnuksen tulisi tapahtua erilaisissa tilanteissa, sekä todentaa, onko sekalajinapa, eli napa, jossa on useaa kestomagneettilajia vain yhden sijasta, käyttökelpoinen sähkökoneissa.

Työssä kehitettiin eksponenttifunktioon perustuva demagnetoitumismalli, jonka voi määrittää vain neljällä parametrilla. Malli ottaa huomioon paitsi hystereesikäyrän pyöreyden, myös magnetointisuuntaa vastaan kohtisuoran demagnetoivan kentän, joka on perinteisesti jätetty huomiotta. Kehitetty malli asennettiin elementtimenetelmämallin osaksi ja testattiin simuloimalla sähkökoneen demagnetoituminen roottorin ollessa lukittuna. Tuloksia verrattiin mittauksiin, jolloin voitiin todeta mallin kykenevän ennustamaan tarkasti magneettien demagnetoitumisen sähkökoneessa.

NdFeB-magneettimateriaalin resistiivisyys mitattiin lämpötilan funktiona. Resistiivisyyden todettiin olevan anisotrooppinen. Työssä todistettiin laskennallisesti, että pyörrevirtamallinnuksessa resistiivisyyttä voi kuitenkin pitää isotrooppisena suureena, kunhan resistiivisyydelle käytetään magnetointisuuntaa vastaan kohtisuoran resistiivisyyden arvoa.

Työssä kehitetty pyörrevirtamalli muuttaa resistiivisyyttä lämpötilan ja magneetin muodon funktiona. Muodon funktiona tehtävän muutoksen todettiin parantavan kaksiulotteisen pyörrevirtalaskennan tarkkuutta.

Demagnetoitumislaskennan suorittamistapaa pohdittiin mallintamalla ylikuumenneen vakiokuormalla kuormitetun moottorin demagnetoituminen. Laskujen perusteella saatettiin todeta lämpömallin käytön olevan oleellinen osa demagnetoitumisen mallintamista.

Sekalajinapaa käytettiin laskuesimerkkinä. Todennettiin, että sekalajinapa parantaa hieman koneen suorituskykyä mahdollistaen samalla kustannussäästöjä.

Acknowledgements

Contents

List of Publications

This dissertation consists of an overview and of the following publications, which are referred to in the text using their symbols:

P1.   Ruoho, S., Dlala, E., Arkkio, A.,
       "Comparison of Demagnetization Models for Finite-Element Analysis of
       Permanent Magnet Synchronous Machines",
       IEEE Trans. Magn., vol. 43, No. 11, pp. 3964-3968, November 2007.

P2.   Ruoho, S., Arkkio, A.,
       "Mixed-Grade Pole Design for Permanent Magnet Synchronous Machines",
       In Proc. of ACEMP'07 and ELECTROMOTION'07 Joint meeting, Bodrum,
       Turkey, 10-12 September 2007, pp. 452-456.

P3.   Ruoho, S.,
       "A Mathematical Method to Describe Recoil Behavior of Nd-Fe-B-Material",
       Seminar presentation, Advanced Magnetic Materials and their Applications
       2007, Pori, Finland, 09-11 October 2007, available online:
       www.prizz.fi/magnettechnology.

P4.   Ruoho, S., Arkkio, A.,
       "Partial demagnetization of permanent magnets in electrical machines caused by
       an inclined field",
       IEEE Trans. Magn., vol. 44, no. 7, pp. 1773-1778, July 2008.

P5.   Ruoho, S., Haavisto, M., Takala, E., Santa-Nokki, T., Paju, M.,
       "Temperature Dependence of Resistivity of Sintered Rare-Earth Permanent
       Magnet Materials",
       IEEE Trans. Magn., vol. 46, No. 1, pp. 15-20, January 2010.

P6.   Ruoho, S., Santa-Nokki, T., Kolehmainen, J., Arkkio, A.,
        "Modeling Magnet Length In 2-D Finite-Element Analysis of Electric
        Machines",
        IEEE Trans. Magn., vol. 45, No. 8, pp. 3114-3120, August 2009.

P7.   Ruoho, S., Kolehmainen, J., Ikäheimo, J.,
        "Anisotropy of resistivity of Nd-Fe-B magnets—Consequences in eddy-current
        calculations",
        in Conf. Proc. REPM08, August 2008, pp. 87-90.

P8.   Ruoho, S., Kolehmainen, J., Ikäheimo, J., Arkkio, A.,
        "Demagnetization Testing for a Mixed-Grade Dovetail Permanent-Magnet
        Machine",
        IEEE Trans. Magn., vol. 45, No. 9, pp. 3284-3289, September 2009.

P9.   Ruoho, S., Kolehmainen, J., Ikäheimo, J., Arkkio, A.,
        "Interdependence of Demagnetization, Loading and Temperature-Rise in a
        Permanent-Magnet Synchronous Motor",
        IEEE Trans. Magn., vol. 46, No. 3, pp. 949-953, March 2010.

List of Symbols and Abbreviations

Symbols

a_1, a_2, a_3	parameters used in the inclined field demagnetization model
B	magnetic flux density [T]
B_r	remanence of a permanent magnet material [T]
$_BH_c$	normal coercivity of a permanent magnet material [A/m]
h	thickness of a permanent magnet, the dimension of a permanent magnet parallel to the magnetization direction [m]
H	magnetic field strength [A/m]
$H_{k, 90\%}$	the value of the magnetic field strength at which the magnetic polarization of a permanent magnet has 90% of its original saturated value [A/m]
I	current, e.g. stator current [A]
J	magnetic polarization of a permanent magnet [T]
$_JH_c$	intrinsic coercivity of a permanent magnet material [A/m]
$_JH_c^{ANG}$	parameter used in the inclined field demagnetization model modified intrinsic coercivity of a permanent magnet material [A/m]
K_1	a parameter used in hysteresis curve calculation representing curve squareness [m/A]
K_2	a parameter used in hysteresis curve calculation [A/m]
L	permanent magnet length, the dimension of a permanent magnet parallel to the length of a permanent magnet machine [m]
M	magnetization [A/m]

N	number of turns in a winding
S	magnetic viscosity constant [A/m]
t	time [s]
T	temperature; a subscript states the point of temperature, e.g., T_{rotor}, rotor temperature [K, ˚C]
V	volume of a permanent magnet [m^3]
w	width of a permanent magnet [m]

μ	permeability [V s m^{-1} A^{-1}]
μ_0	permeability of free space, natural constant, value: $4\,\pi \cdot 10^{-7}$ V s m^{-1} A^{-1}
μ_r	relative permeability [-]
ρ	resistivity, subscript indicates the material [Ωm]
φ	angle between the demagnetizing field and the direction of magnetization, used in the inclined field demagnetization model [°]

Abbreviations

2D	Two-dimensional
3D	Three-dimensional
BLDC	Brushless direct-current machine,
	electronically commutated DC machine, a type of electric machine
Co	Cobalt, a transition metal used in SmCo magnets
Dy	Dysprosium, a metallic rare earth element used in NdFeB magnets
EMF	Electro-Motive Force [V]
FE	Finite Element
FEM	Finite Element Method
MMF	Magneto Motive Force [A]
Nd	Neodymium, a metallic rare earth element used in NdFeB magnets
NdFeB	Neodymiun Iron Boron, a type of rare earth magnet material
P_i	for example: P1, P2,… P9, publications within this study
PM	Permanent Magnet
Pr	Praseodymium, a metallic rare earth element used in NdFeB magnets
Sm	Samarium, a metallic a rare earth element used in SmCo magnets
SmCo	Samarium Cobalt, a type of rare earth magnet material
Tb	Terbium, a metallic rare earth element used in NdFeB magnets

Definition of Terms

Demagnetization

A loss of EMF in an electric machine.

The demagnetization of permanent magnets in an electric machine can be defined by measuring the open-circuit EMF of the machine while the machine is rotating at its nominal speed and comparing that value with the original value of the EMF. The relative drop in the EMF is defined as the demagnetization in this study.

or

The loss of magnetic polarization in a permanent magnet.

The demagnetization of a permanent magnet can be defined by measuring the total magnetic moment of a magnet and comparing the value to the value of the same magnet when saturated. The relative drop in the total magnetic moment is proportional to the relative drop in the magnetic polarization. In this study, the relative drop is defined as the demagnetization.

The two definitions above give the same results in a linear system.

End-Effect

A 3D system can be modeled in two dimensions, if the system remains similar along one axis for some distance. In this case, a 2D model is a cut of the real 3D geometry perpendicular to the axis. In a 2D model, the geometry is assumed to have an infinite length perpendicular to the plane being modeled, and all the physical quantities are calculated against the unit length. The 2D calculation thus ignores the phenomena at the ends of the real finite geometry. These ignored phenomena are called end-effects.

Inclined Demagnetization Model

Normally, it is assumed that only a magnetic field component anti-parallel to the direction of magnetization can cause demagnetization. In reality, the

perpendicular component will also cause demagnetization. An inclined demagnetization model can also take the perpendicular magnetic field component into account.

Linear Magnet Material

A magnet material is called a linear material if the *BH* curve of the material is a straight line through the second quadrant of the hysteresis curve. Sintered NdFeB, SmCo, and some anisotropic hard ferrites are linear materials.

Load Line

A line drawn to the second quadrant of a hysteresis curve. The angle of the line is defined by the geometry of a magnetic circuit. The point of intersection with the horizontal axis is defined by the currents in the magnetic circuit. The load line can be used to study the behavior of a permanent magnet in a magnetic circuit.

Magnet Material

Permanent magnets can be made of different materials. One magnet material has a well-defined microstructure and chemical composition. Modern permanent magnet materials include ferrites, AlNiCos, SmCo-based materials, and NdFeB materials.

Magnet Grade

The chemical composition of a magnet material can be adjusted to produce different magnetic properties. Magnets made of the same material, but of a different alloy composition with different properties, are called magnets of different magnet grades of the same magnet material.

Mixed-Grade Pole

Normally, a pole of a permanent magnet machine consists only of one magnet grade. In a mixed-grade pole, several magnet materials are used in one pole.

Orientation Direction

Modern rare earth magnets are anisotropic. It is possible to magnetize these magnets only in one direction. This direction is prepared by aligning the individual particles in the pressing stage of manufacturing. The direction along which rare earth magnets can be magnetized is called the orientation direction. If the magnet is magnetized, the expression "magnetization direction" can also be used.

Rare Earth Magnets

NdFeB and SmCo magnets are called rare earth magnets.

Rare Earth Metals

A group of sixteen basic elements in the periodic system, also known as Lanthanides, can be found in the same ores. The following rare earth metals are important in the manufacturing of rare earth permanent magnets: Nd, Pr, Dy, Tb, and Sm.

Single-Grade Pole

A pole of a permanent magnet machine, where only one magnet grade is used.

Squareness

An intrinsic hysteresis curve (JH curve) of magnet material curves downwards in the second quadrant of the hysteresis loop. In a material with good squareness the curve is sharp. In a material with bad squareness, the curve is round. The term "squareness" is used when JH curves are being considered. If BH curves are being considered, the term "roundness", which means the same, can be used instead.

Working point

An intersection of the load line and a hysteresis curve (BH curve). The working point gives the magnetic flux density through a permanent magnet in the magnetic circuit under study.

1 Introduction

The introduction of NdFeB magnets in the 'eighties made it possible for permanent magnet machines to come into wider use from the 'nineties onwards. Finnish companies and universities were in the vanguard of utilizing this new technology, mainly because the following necessary factors existed in Finland: experienced companies manufacturing electric machines, universities with a high level of knowledge of electrical engineering and metallurgy, and a large company, Outokumpu Oy, that was capable of starting magnet manufacturing as early as in the 'eighties.

An electric machine is a complex device requiring the knowledge of many areas of science on the part of designers. Knowledge about the permanent magnet material is just a small part of the knowledge required of an electrical engineer. Material scientists, on the other hand know a lot about the properties of permanent magnets, but they do not generally know what is important for electrical engineers. Generally, the link between material scientists and electrical engineers in the scientific community is insufficient. Thus, there are many important concepts which are familiar and trivial to material scientists that are not necessarily known to electrical engineers. This research endeavors to be a bridge between electrical engineering and material sciences. The properties of the NdFeB magnet material are brought closely to the modeling of the machine.

The main focus in this study is on demagnetization modeling. Permanent magnet machines are designed to remain fully magnetized in all working conditions. Still, the machine can sometimes be demagnetized by a fault, overheating or overloading. From the machine user's point of view it is important to be able to calculate the properties of a permanent magnet machine after irreversible demagnetization. From an engineering point of view is interesting to simulate what happens during the demagnetization. In this work, a demagnetization model that is able to calculate the above-mentioned phenomena will be presented.

The magnetic properties of the permanent magnet material are temperature-dependent, which is taken into account in this study. The temperature dependency makes it important to have a thermal model of the machine linked to the electromagnetic modeling. A simple thermal model is used in this study as an example. The losses of the machine need to be accurately calculated to make the thermal model give accurate results. Thus, eddy current loss calculation accuracy within 2D analysis is also improved within this work.

A new pole construction is also introduced. With the new pole structure the properties of a permanent magnet machine can be improved while there is at the same time potential for cost savings. The new construction is evaluated using the demagnetization model, which is also tested by causing a real fault in an existing machine and comparing the measured and the calculated demagnetizations.

1.1   Aim of the Work

The objective of this work is to improve the modeling of permanent magnets in the FE analysis of permanent magnet machines, with especial consideration being given to irreversible demagnetization. The goal is to develop a tool that is able to model demagnetization and implement it in the existing 2D FE code created by Helsinki University of Technology. The demagnetization model must be able to simulate what happens in the magnet during the demagnetization, from which parts the magnet is demagnetized, and the performance of the machine after the demagnetization. The tool will include a demagnetization model, a thermal model, and an eddy current model. The thermal model is needed since the properties of permanent magnets are temperature-dependent. An eddy current model must be able to improve the eddy current calculation accuracy with 2D FEM, since permanent magnets are usually a lot shorter than the length of the machine, making the 2D approximation more inaccurate in eddy current modeling than in the modeling of other properties. The calculation accuracy of the tool will be evaluated by tests with an existing machine.

The second goal of this study is to find out how the simulations with the demagnetization model should be performed to get realistic results from the calculations.

The last goal is to evaluate a new pole design idea, a mixed-grade pole design, by using it in the simulations and tests as an example.

1.2   Scientific Contribution

The most important scientific contributions of the study are listed below.

- A new model for modeling the demagnetization of sintered NdFeB magnets and other anisotropic magnets with a nucleation-type coercivity mechanism is presented. The model has temperature-dependent remanence and intrinsic coercivity. The temperature dependence in the model is linear. The squareness of the hysteresis curve of the magnet material can be adjusted. The recoil behavior in the model is linear.

- A mixed-grade pole design idea is presented. Normally, only one permanent magnet material grade is selected to be used in a machine. In a pole of a machine, some parts are less likely to get demagnetized than other parts. A magnet grade with higher remanence and a lower dysprosium content can be used in those parts which are less vulnerable to demagnetization. With this arrangement, the average dysprosium content of the pole can be optimized, thus offering a potential for cost savings, while at the same time the pole creates a higher flux.

- The recoil behavior of sintered NdFeB material is measured and presented. It is shown that the recoil curve in the second quadrant is not a straight line, but it bends slightly upwards near the B-axis. It is also shown that the recoil curve

does not form a loop if the B-axis is not crossed during the recoil operation. A recoil curve is shown to be capable of being modeled with a straight line with small values of demagnetization.

- Traditionally, only the component of the demagnetizing magnetic field which is anti-parallel to the magnetization direction of the permanent magnet is taken into account when the demagnetization is modeled. In this research, the demagnetization properties of three axially pressed sintered NdFeB material samples are measured with different inclination angles. A simple model is developed to include the perpendicular component of the demagnetizing field in addition to the anti-parallel component, in the demagnetization calculations. The new demagnetization model presented at the beginning of this research is improved by this new property.

- The temperature dependence of the resistivity of commercial rare earth magnets is measured. The measured materials are $SmCo_5$, Sm_2Co_{17}, and NdFeB. Several magnet grades of NdFeB material are measured. The resistivity values of the measured materials are presented over a temperature range $-40\ °C…+150\ °C$. The resistivity values are given both in the orientation direction and perpendicular to the orientation direction. A significant difference in the resistivity in the two above-mentioned directions is observed.

- A new method to improve the eddy current calculation accuracy with 2D FEM by adjusting the resistivity of the magnet material according to the magnet dimensions is presented. Three analytical models are derived from the Maxwell equations. A model based on curve fitting is also presented. All four models are shown to improve the eddy current calculation accuracy.

- By comparing the results of the calculations of eddy currents in the permanent magnets of an electric machine, it is shown that there is a significant difference between the results obtained with 2D and 3D calculations. It is also shown that

the anisotropy of the resistivity of the permanent magnet material must be taken into account only in simulations where a high level of accuracy is required.

- The demagnetization model developed in the course of this study was tested in a real situation. This was the first time that a demagnetization model had been tested with a real motor. A special buried magnet machine was used in the testing with single-grade and mixed-grade poles. According to the tests, the model can predict demagnetization with a good accuracy.

- The dynamics of the demagnetization were studied. It was shown that it is important to include a thermal model of the machine in demagnetization modeling to get accurate results. It was also shown that the demagnetization of a machine loaded by a constant torque has to be calculated in an iterative way.

1.3 Structure of the Work

This dissertation has the following structure.

- Chapter 1 presents the aim and the scientific contribution of the work. The publications written during the course of the work are listed.

- Chapter 2 presents the literature study performed for this research. The properties of the permanent magnet materials are presented and the basics of the demagnetization modeling are discussed.

- Chapter 3 presents the models developed in this study. The focus is on the demagnetization model, while the eddy current model and the thermal model are considered as supportive tools.

- Chapter 4 presents the evaluation of the model. A mixed-grade pole design is presented as an example.

- The discussion and final considerations of the model are given in Chapter 5.

- The references and the literature used as references in this dissertation are listed after Chapter 5.

- The publications and papers included in this dissertation are reprinted at the end of this dissertation.

1.4   Publications

Publication 1

Ruoho, S., Dlala, E., Arkkio, A., "Comparison of Demagnetization Models for Finite-Element Analysis of Permanent Magnet Synchronous Machines", IEEE Trans. Magn., vol. 43, No. 11, pp. 3964-3968, November 2007.

In this paper, the accuracy of some demagnetization models is compared. First, simple demagnetization models found in the literature are presented. The measured recoil behavior and the temperature dependence of the remanence and intrinsic coercivity of the sintered NdFeB material are shown. A new simple exponent function-based demagnetization model is presented. A hysteresis model developed to model hysteresis in soft magnetic material is also shown.

The demagnetization models are compared by modeling the demagnetization of an overloaded and overheated motor with an FEM model. The exponential model gives the most accurate results, because it can easily be adjusted to reproduce the measured hysteresis curve of an NdFeB magnet.

The paper was prepared by Sami Ruoho in co-operation with Emad Dlala, who contributed to the work by including his hysteresis model in the work. Antero Arkkio was the supervisor of the work. The work of Sami Ruoho contributed approximately 80 % of the total work involved in the writing of this paper.

Publication 2

Ruoho, S., Arkkio, A., "Mixed-Grade Pole Design for Permanent Magnet Synchronous Machines", In Proc. of ACEMP'07 and ELECTROMOTION'07 Joint meeting, Bodrum, Turkey, 10-12 September 2007, pp. 452-456.

A permanent magnet machine is traditionally designed to have the magnets manufactured with only one magnet grade. In this paper, a new design idea is introduced: a mixed-grade pole. In a mixed-grade pole, there can be more than one magnet grade in one pole. This structure offers improved resistance against demagnetizing situations, an increased flux produced by the pole and also optimized use of the rare earth metal dysprosium in the magnets, thus creating a potential for cost savings.

The new design idea is modeled and compared with the traditional one-grade design. The benefits of the new pole structure are discussed.

The publication was written and presented in Bodrum, Turkey by Sami Ruoho. Antero Arkkio was the supervisor of the work.

Publication 3

Ruoho, S., "A Mathematical Method to Describe Recoil Behavior of Nd-Fe-B-Material", Advanced Magnetic Materials and their Applications 2007, Pori, Finland, 09-11 October 2007, available online: www.prizz.fi/magnettechnology.

This publication first describes the recoil behavior of partially demagnetized sintered NdFeB magnets. It is shown that the recoil curve of an NdFeB magnet is not a straight line, but bends slightly upwards in the second quadrant near the B-axis. It is also shown that the recoil behavior is almost reversible: the recoil curve shows no loop, if the B-axis is not crossed in the recoil operation.

A new model based on third-degree polynomials is presented to describe the second quadrant recoil behavior of the NdFeB material. The model describes the recoil behavior accurately when the demagnetization is between 0% and 75%. It is also shown that if the demagnetization is below 5%, the recoil curve can be treated as a straight line.

The publication was written and presented in Pori, Finland by Sami Ruoho.

Publication 4

Ruoho, S., Arkkio, A., "Partial demagnetization of permanent magnets in electrical machines caused by an inclined field", IEEE Trans. Magn., vol. 44, no. 7, pp. 1773-1778, July 2008.

This paper develops further the demagnetization model presented in P1. The original model only took into account the demagnetizing field anti-parallel to the magnetizing direction. The improved model also takes into account the demagnetizing field component perpendicular to the magnetizing direction.

A large number of measurements were made for this model. The demagnetization behavior of anisotropic sintered NdFeB magnets of different grades was measured with pulse field measurements. From the measurement results, a simple empirical model was derived that described the demagnetization as a function of the demagnetization field strength and the angle of the demagnetizing field respective to the magnetization direction.

The demagnetization of a simple surface magnet machine and a two-pole high-speed machine is calculated using the model that was developed. It is shown that it is necessary also to consider the perpendicular demagnetizing field component in accurate demagnetization calculations.

The paper was written by Sami Ruoho. Antero Arkkio was the supervisor of the work.

Publication 5

Ruoho, S., Haavisto, M., Takala, E., Santa-Nokki, T., Paju, M., "Temperature Dependence of Resistivity of Sintered Rare-Earth Permanent Magnet Materials", IEEE Trans. Magn., vol. 46, No. 1, pp. 15-20, January 2010.

In all available standards the resistivity of rare earth magnets is given as a single value. No information is given about the temperature coefficients or the effect of magnetization. Modern rare earth magnets have an anisotropic crystal structure, so it was also necessary to measure their resistivity in different directions.

In P5, the resistivity of three rare earth permanent magnet materials ($SmCo_5$, Sm_2Co_{17}, and $Nd_2Fe_{14}B$) was studied. The resistivity was measured over the temperature range which covers most situations in modern industrial permanent magnet machines: -40 °C…+150 °C. The measured resistivities and their temperature coefficients are reported. The resistivity was also measured using magnetized and non-magnetized samples. Within the measurement accuracy, these results were the same. When the

resistivity was measured along the orientation direction and perpendicular to the orientation direction, a large difference was detected showing anisotropy in resistivity too. The anisotropy of resistivity must be taken into account in the eddy current calculations of rare earth magnets.

The paper was prepared in cooperation with other authors. All the authors contributed to defining the measurement problem and the actual writing of the paper. Sami Ruoho acted as a contact writer. Sami Ruoho contributed by getting and preparing the samples, handling the results, and drawing the conclusions on the basis of the results. Minna Haavisto contributed by making the measurements and pre-handling the results. Eelis Takala contributed by making the measurements and by estimating the measurement accuracy. Timo Santa-Nokki contributed the FEM calculations validating the measurement setup. Martti Paju was the supervisor of the work. The work of Sami Ruoho contributed approximately 45 % of the total work involved in writing of this paper.

Publication 6

Ruoho, S., Santa-Nokki, T., Kolehmainen, J., Arkkio, A., "Modeling Magnet Length In 2-D Finite-Element Analysis of Electric Machines", IEEE Trans. Magn., vol. 45, No. 8, pp. 3114-3120, August 2009.

Electric machines are usually modeled with 2D FEM calculations rather than the more accurate 3D calculations because of the faster calculation time and simpler problem definition. The 2D calculations cannot take into account the end-effects of the machine geometry, which cause a large error when eddy current losses in permanent magnets are being calculated.

Three analytical models are derived and one model based on the curve fitting is developed to improve the accuracy of 2D eddy current calculations. In all the models, the resistivity is adjusted according to the dimensions of the magnet. The temperature

dependence and the anisotropy of the resistivity are also taken into account. The models are compared against 2D and 3D eddy current calculations. It is shown that all the models that are presented improve the accuracy of the eddy current calculation in 2D.

The paper was prepared in cooperation with other authors. It was mainly written by Sami Ruoho. The analytical models and the curve-fitting models were developed by Sami Ruoho. Timo Santa-Nokki contributed by making a huge number of simulations with a commercial FEM software package for the curve-fitting model. Jere Kolehmainen contributed by performing the FEM simulations used to validate the model. Antero Arkkio was the supervisor of the work. The work of Sami Ruoho contributed approximately 45% of the total work involved in the writing of this paper.

Publication 7

Ruoho, S., Kolehmainen, J., Ikäheimo, J., "Anisotropy of resistivity of Nd-Fe-B magnets — Consequences in eddy-current calculations," in Conf. Proc. REPM08, August 2008, pp. 87-90.

The resistivity of NdFeB material is anisotropic. The value of resistivity perpendicular to the orientation direction of the magnet is smaller than the value of resistivity in the orientation direction. In this paper, eddy current losses in the permanent magnets of a permanent magnet machine are modeled in three cases: 2D, 3D with isotropic resistivity and 3D with anisotropic resistivity. It is shown that there is a significant difference in the results between 2D and 3D calculations. The anisotropy of resistivity has to be taken into account only if very high accuracy is required in the eddy current calculations.

The publication was prepared in co-operation with other authors. It was mainly written by Sami Ruoho. It was presented in Crete by Sami Ruoho. Jere Kolehmainen contributed by performing the FEM simulations. Jouni Ikäheimo was the supervisor of the work. The work of Sami Ruoho contributed approximately 45 % of the total work involved in the writing of this publication.

Publication 8

The demagnetization of a special buried magnet machine geometry, a dovetail machine, is modeled in a locked rotor situation at a high temperature. Poles in a dovetail machine have several magnets, making it ideal for a mixed-grade pole design. Both single-grade and mixed-grade configurations are modeled. The modeled situations and magnet configurations are tested with a real motor. By comparing the test results and the calculations, it can be shown that the demagnetization model used can predict the demagnetization with good accuracy.

The paper was prepared in cooperation with other writers. It was mainly written by Sami Ruoho. Sami Ruoho contributed to the manufacturing of the magnets, performing the necessary simulations and taking part in the testing. Jere Kolehmainen contributed by doing most of the testing. Jouni Ikäheimo contributed by arranging the testing facilities. Antero Arkkio was the supervisor of the work. The work of Sami Ruoho contributed approximately 50 % of the total work involved in the writing of this paper.

Publication 9

Ruoho, S., Kolehmainen, J., Ikäheimo, J., Arkkio, A., "Interdependence of Demagnetization, Loading and Temperature-Rise in a Permanent-Magnet Synchronous Motor", IEEE Trans. Magn., vol. 46, No. 3, pp. 949-953, March 2010.

The dynamics of the demagnetization are studied in this paper. A dovetail machine with a constant load torque is modeled. A slight demagnetization in a machine running under a constant torque will cause an increase in the load angle, which will cause an increase in the resistive losses of the stator. The increased losses will increase the temperatures inside the machine. This can again lead to additional demagnetization, which will again increase the losses. In some cases, this process will go on until the machine stalls.

In this paper it is shown that a thermal model of the machine must be included for accurate demagnetization modeling, because the demagnetization will cause an increase in the machine temperatures. An iterative approach to demagnetization modeling is shown.

The paper was prepared in cooperation with other authors. It was written by Sami Ruoho. Jere Kolehmainen contributed by allowing the use of the machine design developed by him. Jouni Ikäheimo contributed by giving the basic idea for this research: the idea of drifting demagnetization. Antero Arkkio was the supervisor of the work. The work of Sami Ruoho contributed approximately 85 % of the total work involved in the writing of this paper.

2 Demagnetization Modeling

The behavior of an electric machine is nowadays mostly modeled with a 2D FEM. The cross-section of the machine is divided into elements and the magnetic vector potential is solved at nodal points of the elements. The magnetic flux density and the other quantities at each point of the cross-section of the machine can be calculated from the nodal vector potential.

In an FE model, materials mostly have linear properties: only the magnetic properties of soft iron in a machine are normally modeled with a non-linear model. The properties of the permanent magnets are also modeled with a linear model. With modern magnet materials, this can be enough, if the magnet is not stressed too much magnetically. However, if the partial demagnetization needs to be modeled, a linear model of a permanent magnet is not sufficient.

Normally, a permanent magnet machine is designed to survive the most difficult conditions a designer might think are possible without demagnetization. In these cases, the designer can use a linear model of a permanent magnet in modeling, and only check afterwards the worst working point inside the magnets. If the worst working point does not show a risk of demagnetization, the design can be accepted.

In some cases a machine might experience very rough working conditions. In cases such as a loss of cooling or short circuits, the magnets in a machine might be magnetically so stressed that they become partially demagnetized. The performance of the machine after a fault situation needs to be calculated. The behavior of the machine during the fault is also interesting. A demagnetization model which can simulate permanent magnet behavior realistically is needed in these calculations. A good model will also help a designer to select the permanent magnet material correctly in order to avoid partial demagnetization.

When this research was started in 2006, the commercial FEM software for the electromagnetic modeling of permanent magnet machines mostly used linear models for magnetic materials, in which the characteristics of the permanent magnet were set with a few constant parameters. Now, in 2010, the commercial software packages have become more sophisticated in modeling permanent magnet materials: some solvers can model both magnetization and demagnetization (Allcock, 2009). The shape of the *BH* curve can be defined either by some simple parameters or by splines (Lombard, 2009). However, some available definitions might be quite complex to use, and thus to model the behavior of permanent magnets accurately the modeler must act in close cooperation with experts on permanent magnet materials. Some companies supplying software have developed their demagnetization models in close cooperation with manufacturers of permanent magnets. Some companies are currently developing material databases together with the material manufacturers.

2.1   Properties of PM Materials

2.1.1   Permanent Magnet Materials

When the theory of electromagnetism was formulated in the nineteenth century, the only permanent magnet materials that existed had quite poor properties. All the important permanent magnet materials currently in use were discovered during the 20th century: AlNiCo magnets were discovered in the 'thirties. These magnets still have some use because of their high remanence, high operating temperatures, good temperature stability, and good corrosion resistance. The next material to be discovered was the ferrite magnet. The hard ferrites are widely used because of their low cost. Modern ferrite magnets are linear but have relatively low remanence. The ferrites are ceramic and thus they do not conduct electricity, which is an important feature in many applications.

In the 'seventies rare earth magnets were discovered. The first rare earth magnet to be introduced was $SmCo_5$. Later in the 'seventies Sm_2Co_{17} was introduced. Both these magnets have high remanence, high corrosion resistance, and relatively high maximum operating temperatures. A drawback of these magnets is their composition: SmCo magnets are quite expensive because of the high price of cobalt.

At the beginning of the 'eighties another magnet material was introduced into the rare earth family: NdFeB magnets. These magnets have the highest available remanence, and, like SmCo magnets, they have linear behavior. NdFeB magnets are prone to corrosion. This is a major drawback of these magnets, meaning that they must be protected in many applications by coating. NdFeB magnets are brittle, which means that they require careful handling and special attachment methods in applications. Like SmCo magnets, NdFeB magnets are electrically conductive materials, making it necessary to consider eddy current losses in the magnets.

The magnetic properties of the permanent magnet materials needed in electric machine modeling can be defined with four main parameters: remanence (B_r), intrinsic coercivity ($_JH_c$), recoil permeability (μ_r), and the squareness of the hysteresis curve. Another parameter which is very often given is normal coercivity ($_BH_c$). Normal coercivity can be understood as a consequence of remanence and the recoil permeability. The Maximum Energy Product $(BH)_{max}$ is also often given, but in modern linear materials it can be exclusively calculated from remanence (Outokumpu, 1990)

$$(BH)_{max} = \frac{B_r^2}{4\mu_0\mu_r}.$$
(2.1)

Remanence describes the strength of the magnet. Intrinsic coercivity describes the ability of the magnet to remain fully magnetized in an opposing magnetic field. Recoil permeability shows the slope of the *BH* curve. Squareness defines the quality of the *JH* curve, good magnets have a square corner in their *JH* curve in the third quadrant, while poor magnets have a round corner.

The magnetic properties of the permanent magnet material are often presented with hysteresis curves. Normally, only the second quadrant of the hysteresis loop is given. Because the magnetic properties are dependent on the temperature, the curves are usually given both at room temperature and at elevated temperatures. Two types of curves are given: the flux density through the magnet as a function of the magnetic field (*BH* curves) and the magnetic polarization as a function of the magnetic field (*JH* curves). Each point on a *JH* curve (H_m, J_m) can be related to a corresponding point on the *BH* curve (H_m, B_m)

$$B_m = \mu_0 H_m + J_m .$$ (2.2)

An example of hysteresis curves can be found in Fig 2.1.
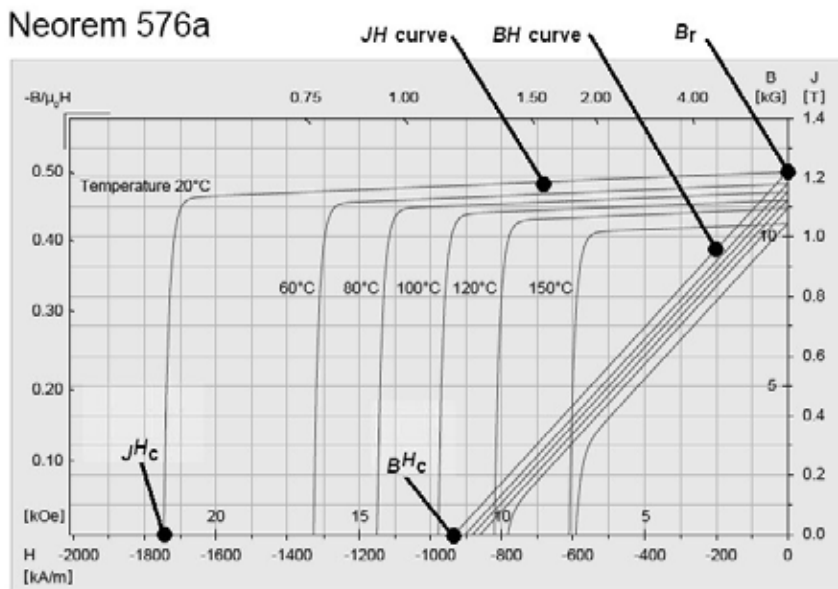
Fig. 2.1 A hysteresis curve of a sintered NdFeB magnet material (Neorem Magnet, 2010).

2.1.2   Sintered NdFeB Magnet Material

This research concentrates on modeling sintered NdFeB magnet material, which is the latest development in permanent magnet materials. It has the highest available remanence and energy density. The material also shows very high intrinsic coercivity, especially at room temperature. Both intrinsic coercivity and remanence have negative temperature coefficients, meaning that the properties of this magnet material degrade as the temperature rises. The maximum working temperature of NdFeB magnets depends on the application and on the magnet grade. Some magnet grades can be used at room temperature only. Some NdFeB grades can be used up to 200 ℃.

An NdFeB material has the following basic chemical composition: 30-32% of its weight is rare earth metals, 1% of its weight is boron, 0-3% of its weight is cobalt, and the balance is iron. There are also minor quantities of metals like copper in the alloy for metallurgical reasons. There can be different rare earth metals in the alloy. The most commonly used metals are: neodymium (Nd), dysprosium (Dy), praseodymium (Pr) and terbium (Tb). Nd and Pr are called light rare earths, while Dy and Tb are called heavy rare earths. For the time being, most of the rare earth metals are supplied by China (Kennedy, 2009), but there are also important projects in, for instance, the USA, Canada, Australia, and South Africa.

Different magnet grades of NdFeB magnet material are manufactured by changing the relative quantities of the rare earth metals. In a basic NdFeB magnet only Nd and Dy rare earths are present. If the Nd content is high and the Dy content is low, the magnet has a high remanence (more than 1.3 T) and a low intrinsic coercivity (around 1000 kA/m). If the Dy content is increased, the remanence will drop, but the intrinsic coercivity will rise considerably. In Fig 2.2 it is possible to see how the remanence increases and the intrinsic coercivity drops as the relative Dy content decreases.
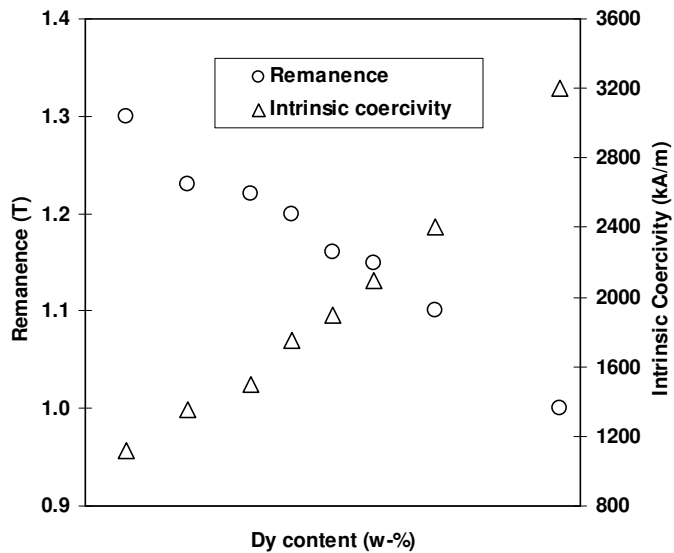
Fig. 2.2 The properties of a series of axially pressed magnet grades as a function of the Dy content of these magnet grades.

Dysprosium is more expensive than neodymium. In recent years the price difference between these two metals has become larger, as can be seen in Fig 2.3. It means that magnet grades with a higher dysprosium content have a higher price/kg than magnet grades with a lower dysprosium content. In other words, the magnet grades with higher intrinsic coercivity are more expensive than the magnet grades with high remanence. This means that the selection of the magnet grade for an application is a complex optimization problem that involves both the magnetic properties and the price.
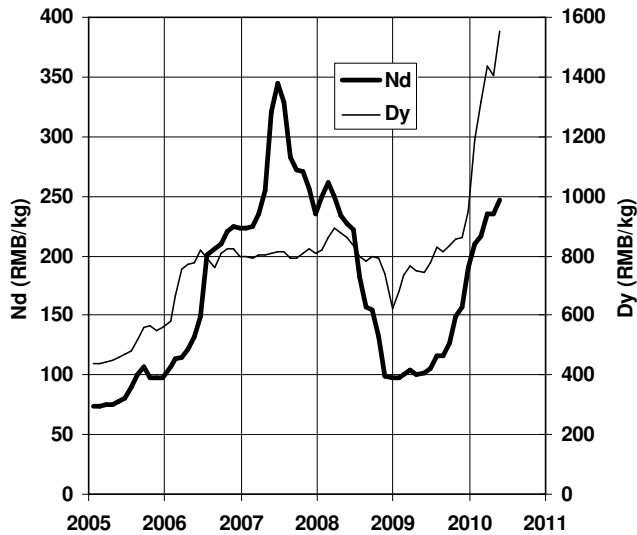
Fig. 2.3 The price development of neodymium and dysprosium (Asianmetal).

Since NdFeB magnets were discovered quite recently, there are still many patents covering the composition, structure, or manufacturing of the material. Most patents are owned by Hitachi Special Metals, which has made license agreements with certain manufacturers. The products of these licensees of Hitachi Special Metals are called licensed magnets. Only licensed NdFeB magnets can be used in products, which are intended for export to countries where the patents are valid (Hitachi Special Metals, 2007).

2.2   Demagnetization of Permanent Magnet Material

The magnetic conditions of a single point of a fully saturated permanent magnet in a magnetic circuit can be described with three values: the magnetic field H_m, magnetic flux density B_m, and magnetic polarization J_m. J_m and B_m are connected as stated before in Equation 2.2. The point on the BH curve defined by the values H_m and B_m is called

the working point. Usually, the working point is slightly different in every part of the magnet. In a transient situation, the working points in the different parts of the magnet might have drastic differences.

In traditional analytical calculations with a parametric model of a magnetic circuit, it is normally assumed that the working point is the same throughout the magnet. In this kind of analysis, a working line can be defined. The slope of the working line is only dependent on the geometry of the magnetic circuit. If there are no currents present in the circuit, the working line goes through the origin. If there are currents present, the working line intersects the H-axis at a point, which is dependent on the thickness of the magnet h_m and on the ampere turns at the magnetic circuit as follows: $-NI/h_m$. The intersection point of the working line and the BH curve is the working point. An example of a working line and a working point can be seen in Fig 2.4.

The risk of demagnetization can be studied easily with the BH curve and the working point. Because of the temperature dependence of the intrinsic coercivity, the BH curve will bend at higher temperatures. Thus, the BH curve will have a linear part with a slope and a vertical part. The area between these parts is called the knee of the BH curve.
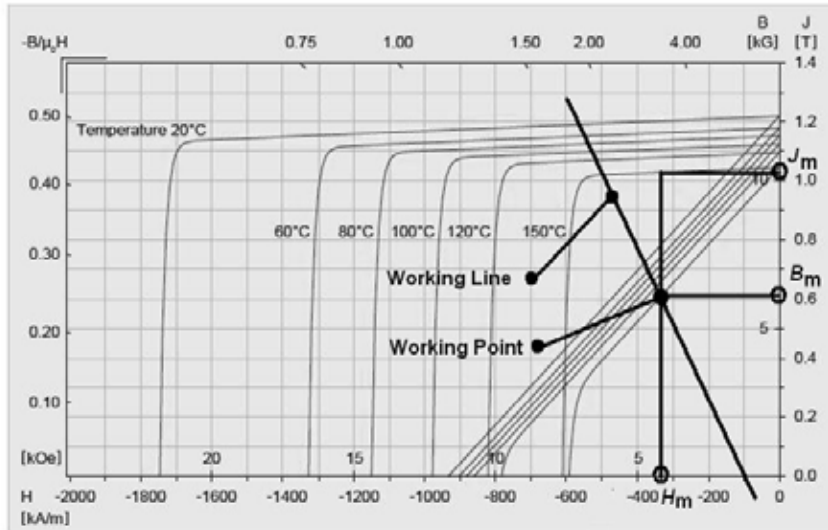
Fig. 2.4 Working line and working point of a magnet at 150°C. The slope of the working line is defined by the machine geometry. The intersection point of the working line and the *H*-axis is defined by the thickness of the magnet and number of ampere turns in the magnetic circuit: -*NI*/*h*$_\mathrm{m}$. The intersection between the *BH* curve of the working temperature and the working line is called a working point.

If the working point of the design stays clearly in the linear region, there is no risk of demagnetization. If the working line intercepts the *BH* curve below the knee at the vertical part of the curve, there will be a partial irreversible demagnetization of the permanent magnet. To avoid the risk of partial demagnetization, the designer of the magnetic circuit must ensure that the working point stays well above the knee area of the hysteresis curve in the worst possible conditions.

In a permanent magnet, the working point can move below the knee for two reasons: a temperature that is too high or a current that is too high. Practically, it is not possible to separate whether the demagnetization is caused by a too-high temperature or by a too-high current. High currents can be tolerated at low temperatures and high temperatures

with low loading. An increasing temperature will cause the knee area of the *BH* curve to move rightwards, closer to the vertical *B*-axis. If the loading conditions remain the same, the working line remains the same. At some temperature, the working point will be below the knee and there will be partial demagnetization. After the demagnetization the remanence of the magnet is reduced. A new line, called a recoil line, can be drawn from the lowest working point. If the demagnetization is less than 10%, the slope of the recoil line will be approximately linear. With higher demagnetizations, the recoil line will be slightly bent upwards because of the magnetic domain structure (Sagawa 2007, Kobayashi 2004), as shown in Fig 2.5. After the demagnetization, the recoil line must be used instead of the *BH* curve of the saturated magnet in the working point analysis. In Fig 2.6, a demagnetization caused by increased temperature is presented.
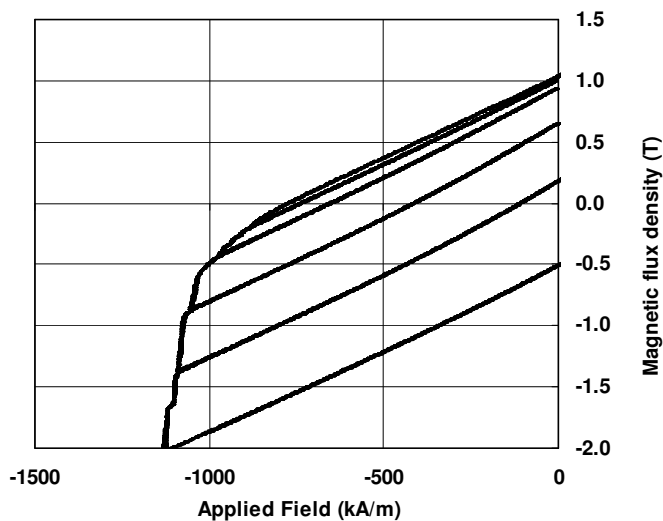
Fig. 2.5 Recoil behavior of NdFeB magnet sample. The recoil curve is bent upwards near the vertical *B*-axis.

Neorem 512a
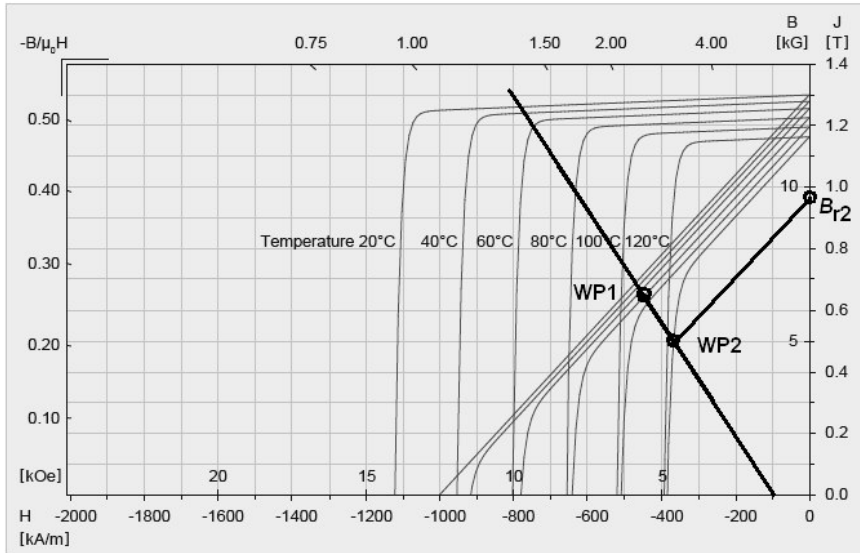
Fig. 2.6 Irreversible demagnetization caused by increased temperature. In this example, the machine is expected to operate at 80 °C at the working point WP1. After the temperature is increased to 120 °C a new working point WP2 exists at the intersection of the load line and the *BH* curve at 120 °C. After the irreversible demagnetization, the remanence at 120 °C drops to the value B_{r2} and the line between WP2 and B_{r2} should be used instead of the *BH* curve to estimate the behavior of the machine.

The working point can also move below the knee as a result of high currents in a machine. There can, for example, be a short circuit. At the very beginning of a short circuit situation, the temperatures remain the same, but the working line is suddenly moved to the left. In this situation, the working point can be below the knee, and demagnetization happens. In Fig 2.7, demagnetization as a result of a high current is presented.

Neorem 512a
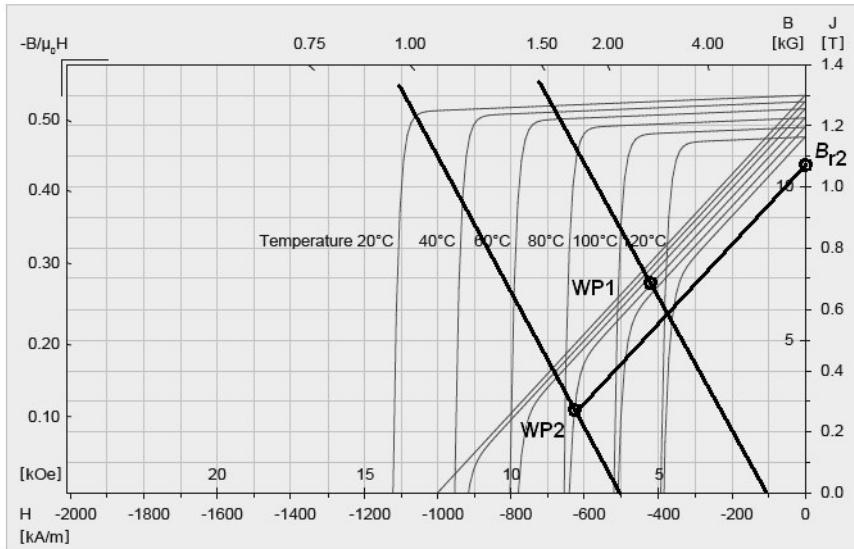
Fig. 2.7 Irreversible demagnetization caused by a too-high current, for example in a short circuit. In this example, the machine is expected to operate at 80 °C at the working point WP1. After a short circuit a new working point WP2 exists at the intersection of the load line and the *BH* curve. After the irreversible demagnetization, the remanence drops to the value B_{r2} and the line between WP2 and B_{r2} should be used instead of the *BH* curve to estimate the behavior of the machine.

2.3   Risky Situations for Demagnetization

Irreversible demagnetization in a permanent magnet machine is caused either by too high a temperature, too-high stator currents, or both. There are several situations which can typically be risky and which the designers should take into account when designing a permanent magnet machine.

Short-circuits are very dangerous from the point of view of the machine, because they will first cause a very high current transient, and, if the machine is kept in operation, they will cause high losses and the temperature will increase. A common type of short

circuit is a phase-to-ground short circuit, i.e. a one-phase short circuit. The most common and the most dangerous short circuit is a phase-to-phase short circuit, i.e. a two-phase short circuit. The damage caused by a two-phase short circuit depends on which part of the electric cycle the short circuit happens in, which makes the modeling of a two-phase short circuit demanding. A three-phase short circuit is important, because it can happen entirely outside the machine, for example inside a frequency converter. Sometimes a frequency converter can be programmed to cause a three-phase short circuit if it detects a two-phase or a one-phase short circuit, because a three-phase short circuit causes the least damage.

If a machine is overheated, the magnets can become irreversibly demagnetized. The overheating can be caused, for example, by a loss of cooling, which must be taken into account in liquid-cooled machines in particular. In some cases the ambient temperature can be exceptionally high, which will also cause high temperatures inside a machine.

Some machines have been designed to be used only every now and then. Between the uses a pause is expected. For example, an elevator motor could be designed like this. A short-duty-cycle machine as described here can have a cooling system adapted for this periodical use. If this kind of machine is running continuously for some reason, the cooling may be insufficient and the machine will overheat.

Eddy currents are difficult to model accurately. If there is a great error in the eddy current calculations, there can be too much losses in a machine. Sometimes the thermal design of a machine is neglected. In these cases the machine must be used below the rated point in order to keep the working point of the magnets in the linear region.

One type of machine, which is very difficult from the point of view of demagnetization is a line-starting machine. This kind of machine can be connected directly to the grid without a frequency converter. These machines usually have a cage winding in addition to permanent magnets. The cage winding will accelerate the rotor of the machine until it synchronizes with the stator field. During the start-up, the working point of the magnets

can have values as low as $B_m = -1$ T. If this kind of machine is started when it is heated up, a very demanding magnet material is needed, or there is a high risk of demagnetization.

2.4 Literature Study

The partial demagnetization of permanent magnets in electric machines has been the subject of interest in many publications in recent years. Several authors have studied the influence of demagnetization on the behavior of a machine. Some authors have studied demagnetization from the point of view of fault diagnostics. Many authors have checked their design to be sure that it will not become demagnetized during a fault. Different demagnetization models have been described in many publications. The models are based on hysteresis models or on linear equations. However, the demagnetization phenomenon itself has not been studied from the point of view of permanent magnet machine. The dynamics of the demagnetization, i.e. how the demagnetization should be modeled to get reliable results, has also been neglected in the previous publications.

2.4.1 Magnet Material

One of the first steps in the design of a permanent magnet machine is the selection of the permanent magnet material. Trout (2001) wrote a good paper about the selection of the correct magnet material for an application. He considered the different properties of magnet materials and whether the properties are useful from the point of view of material science or from the point of view of electrical engineering.

Most modern permanent magnet machines use rare earth magnets. There are three kinds of rare earth magnets: NdFeB magnets, $SmCo_5$ magnets and Sm_2Co_{17} magnets. This study concentrates mostly on NdFeB magnets.

The basic composition of the hard magnetic phase of a sintered NdFeB magnet is $Nd_2Fe_{14}B$. Different magnet grades with different properties can be created by replacing some of the Nd by other rare earth metals and some of the Fe by other transition metals, usually cobalt. The replacement of Nd by Dy is used to increase the intrinsic coercivity of NdFeB material, as shown by Grössinger et al. (1987).

In modern rare earth magnets, the grain size is much larger than the magnetic domain size. For example, the grain size of a sintered NdFeB material is around 10 μm, while the single domain particle size would be only 0.26 μm, according to Jiles (1991). Thus, according to McCaig and Glegg (1987), in an unmagnetized state there are several magnetic domains in a single grain that are anti-parallel to each other in the NdFeB material.

The intrinsic coercivity of the rare earth magnets can be based either on pinning or on nucleation. According to Campbell (1994), the intrinsic coercivity of Sm_2Co_{17} is based on pinning, while the intrinsic coercivity of $SmCo_5$ and sintered NdFeB magnets is based on nucleation. In an unmagnetized NdFeB magnet there are several anti-parallel magnetic domains in a single grain, making the whole magnet magnetically neutral. After the material is magnetized, there will only be one domain in a single grain. If the material suffers partial irreversible demagnetization, there will be three kinds of grains, as described by Kobayashi et al. (2004): grains magnetized in the original magnetization direction, grains magnetized anti-parallel to the original direction of magnetization, i.e., parallel to the direction of the demagnetizing field, and grains which have many domains. These grains with multiple domains act as soft particles and, according to Sagawa (2007), cause the bending of the recoil curve near the B-axis.

2.4.2   Limit of Demagnetization in Electric Machines

There are many publications where the risk of the demagnetization of the design is checked. First, the limit of the demagnetization is defined. Then the lowest working point in the machine is calculated and the value is compared against the limit. In some

publications the checking is performed analytically and in some publications using numerical calculations.

Kang et al. (2000) studied an axial-flux generator. They derived an analytical equation where the lowest possible working point of the magnets in a machine during a fault situation can be calculated. The lowest working point is then compared with the coercivity of the magnets to see if the machine will be demagnetized during the fault. Ooshima et al. (1997) also derived an analytical equation, where the maximum current, which is not yet causing demagnetization, can be calculated using the machine dimensions and the properties of the permanent magnet as parameters. The analytical equation is validated with the FE calculations. In their paper, Arshad et al. (2001) designed a motor for transient applications. Because a motor for a transient application runs only for a short time, the motor dimensioning should not be based on the thermal loading, but the most critical design factor is to avoid demagnetization. The authors present analytical equations for the calculation of the motor dimensions if the smallest possible flux density inside the permanent magnets, i.e., the demagnetization limit, is known. Dorrell and Klauz (2003) introduced a simple optimization routine for a PM commutator machine. They derived an analytical equation for the smallest possible flux density inside a magnet. The magnet weight is optimized in the routine, and the equation gives a limit to the thickness of the magnet. Morimoto et al. (1990) studied the field-weakening operation of a DC motor to achieve higher rotational speeds. The authors stated that the prevention of the demagnetization of the magnet as a result of the direct axis armature current is an important design feature in their application. They defined an analytical equation for the demagnetization limit. The properties of the motor as a function of the rotational speed were also studied with the demagnetization limit being considered. Wang et al. (2008) developed an analytical method to identify the regions of permanent magnets which are the most prone to partial demagnetization. Their model is based on comparing the flux density inside a region in a permanent magnet to a limit set by the user. The model is claimed to be faster than time-stepping FEM calculations. The model takes into account only the field component parallel to the magnetization direction.

2.4.3 Short Circuits

There are several faults that can cause the demagnetization of permanent magnets. Short circuits are obvious electrical faults that can cause demagnetization. There are different kinds of short circuits which are possible in a three-phase machine. Different studies show that two-phase short circuits are the most dangerous. It has also been shown that a machine can be protected from short circuits by designing the structure properly.

Lampola and Saransaari (2000) analyzed several surface magnet machines. They set up a rule for how to limit the maximum loading of the machine according to the demagnetization characteristics. They modeled both three-phase and two-phase short circuits. A temperature limit was set, below which the modeled machines will survive short circuits. They noticed that a two-phase short circuit is more dangerous for the machine than a three-phase short circuit. They also pointed out that the seriousness of a two-phase short circuit depends strongly on the phase angle of the voltages at the time of the short circuit. Goldenberg et al. (1997) studied the minimum flux density inside the magnets of a surface magnet machine during single-phase and six-phase short circuits. They showed that a damping cage can prevent demagnetization in the case of a one-phase short circuit. Thelin (2002) analyzed different short circuits in an inverted-fed buried-magnet synchronous machine. He analyzed one-phase, two-phase, and three-phase short circuits in machine terminals. He also analyzed a short circuit of one of the commutating diodes. The risk of demagnetization was analyzed after each short circuit by checking the lowest flux density inside the magnet material. Rosu et al. (1999) compared a surface-mounted magnet machine to a PM machine with pole shoes. The risk of demagnetization of the machines was checked in cases of maximum loading and one-phase and three-phase short circuits. It was noticed that the corners are the most critical parts of the magnets, because they will demagnetize the most easily. Lampola (1999) studied the optimization of permanent magnet machines with different rotor designs. He studied the demagnetization resistance of the different rotor designs by analyzing the smallest flux density inside the magnets during a three-phase short circuit. He noticed that rotor designs with pole shoes are better protected during a fault.

2.4.4 Fault Diagnostics

If a machine becomes demagnetized, it might be interesting to know the performance of the machine after the demagnetization. This is very important, for example, in applications where the condition of the machine can have an effect on general safety. There are several papers concerning the fault diagnostics and performance analysis of demagnetized machines.

Farooq et al. (2006a) modeled a demagnetized outer rotor synchronous machine with a permeance network model based on the work of Perho (2002). In their model the magnets have uniform magnetization, i.e., all magnets are magnetized and demagnetized homogenously and equally. They suggested some improvements to their model to allow the modeling of such demagnetization, which is not uniform through the magnets. Farooq et al. used their model to study the properties of a partially demagnetized machine. They showed the effect of demagnetization on the shape of EMF and also on torque. The results were verified by FE modeling and measurements. Later Farooq et al. (2006b) used the results of the model in fault analysis. In their method, the EMF is first measured. After that, the remanence in the different regions of permanent magnets is calculated according to the EMF measurement results. The drop in the remanence shows the demagnetization inside the magnets.

Boucherit et al. (2004) used a superposition theorem to model the demagnetization fault of a PM machine. First, the motor is modeled with healthy permanent magnets. After that, the motor is modeled with permanent magnets whose magnetization corresponds to the assumed demagnetization fault. The results are summed to evaluate the resulting shape of the EMF and the air gap flux density. They suggested that their model can be used in the diagnostics of PM machines.

Models have been developed by several research groups to detect demagnetization by analyzing some motor parameters. Xi et al. (2008) developed a model where the demagnetization can be detected by analyzing the Fourier expansion of the motor flux

linkage. The type of demagnetization fault which they analyzed is not described in their paper. Rosero et al. (2006) developed a method based on Fast Fourier Transform (FFT) to detect demagnetization faults. They built motors with magnets which were not fully magnetized during the manufacturing process. After that they analyzed the current waveform with FFT to detect the demagnetization. Later Romero et al. (2008) built another model based on the Hilbert Huang transform and tested it in a similar way. The problem in their testing is that permanent magnets normally do not demagnetize uniformly during a fault. Only uniformly magnetized magnets were used in the testing of Rosero et al.

2.4.5 Hysteresis Models

The behavior of permanent magnet materials is hysteretic, and thus it is natural to try to model the behavior of permanent magnets with hysteresis models. Hysteresis modeling is usually very complex and, to model the exact behavior of a material, several time-consuming measurements have to be carried out. However, the hysteresis phenomena and hysteresis modeling are a widely researched field, and there are several groups in the world studying hysteresis and developing models.

Hysteresis models have been used to model the behavior of soft iron in electric machines. For example, the Preisach model is widely applied in the modeling of hysteresis. Some of the models developed for soft iron have also been applied to the modeling of permanent magnet materials. Rosu et al. (1998) built a model to simulate the hysteretic behavior of NdFeB permanent magnet material. The model was based on Preisach's theory and requires the first-order return curves as fitting parameters. The model was later implemented in an FEM code and used in electric machine modeling. Rosu et al. (2005) used a Preisach-type hysteresis model to simulate the demagnetization of a permanent magnet machine. They repeated the demagnetizing conditions several times and noticed that after the demagnetization, similar conditions do not cause additional demagnetization. In their testing, both two-phase and three-phase short circuits were considered. They stated that a two-phase short circuit is more

common and more dangerous for the machine from the point of view of demagnetization.

Full hysteresis models can model both magnetization and demagnetization. Enokizono et al. (1997) studied the magnetization distribution of a four-pole magnet after magnetization with a pulse magnetizer. They used Variable Magnetization and the Stoner-Wohlfarth method in their calculations. Their model can be used to simulate the magnetization of an anisotropic permanent magnet material in cases, where the magnetizing field is not parallel to the direction of magnetization of the magnet. Later, Enokizono et al. (2003) improved the model so as to be able to take into account the eddy currents induced during the magnetization. This was a great improvement compared to their first model (Enokizono et al. 1994), which could be used only to model magnetization by a static magnetic field. However, the model has not been used to simulate demagnetization. A variable flux memory motor is an interesting application, in which the rotor flux can be controlled by magnetizing and demagnetizing the rotor magnets with current pulses from the stator. This kind of motor was studied by Lee and Hong (2008). They used Preisach's model combined with an FEM tool to simulate the demagnetization and remagnetization of the ferrite magnets in a motor.

An important part of demagnetization modeling with hysteresis models is to study the shapes of the minor hysteresis loops. Phelps and Atherton (2001) developed a model to study the shapes of the minor loops. It is noted that the surface area of the minor loops is very small if the coercivity is not based on pinning. The coercivity of NdFeB magnets is based on nucleation, and thus it can be assumed that the surface area of the minor loops must be small. The latest model of minor loop modeling is that of Harrison (2009). He developed an analytical theory to reproduce first-order return curves. He compared his model against the measurements of both soft and hard magnetic materials.

2.4.6   Simple Linear Demagnetization Models

Hysteresis models are often too difficult to assign in association with complicated machine geometries. They are also heavy to calculate. To make the demagnetization modeling faster, more simple demagnetization models have been developed. Researchers in Korea (Kang, Kim, and Lee) have introduced a two-piece linear model, where the *BH* curve of a ferrite magnet is defined with two lines in the second quadrant of the hysteresis loop. The first line travels from the vertical *B*-axis to the knee point, after which the second line travels down with a higher slope to the horizontal *H*-axis. The demagnetization calculation method is described accurately in their publications. The model is implemented in a 2D FE analysis tool. Each element in permanent magnets is handled separately. The solution is iterated until no more demagnetization happens.

Kang et al. (2003a) described their demagnetization model in their conference paper. They used the model to compare three different BLDC machine topologies using ferrite magnets. The areas in the magnets which are the most prone to demagnetization in the topologies that are presented, are shown. Kang et al. (2003b) optimized a one-phase squirrel-cage line-starting motor based on ferrite magnets using the model. After the optimization they were able to reduce, but not totally remove, the demagnetization of the magnets during the start-up of the machine. Lee et al. (2004) optimized a BLDC motor for traction applications using the model. They studied the demagnetization of the ferrite magnets during the start-up transient and compared the behavior of two machine topologies. Later Kim et al. (2006) used the same model to simulate a traction motor with sintered NdFeB magnets. They optimized the shape of the magnet pole and calculated the EMF, cogging torque, and load angle curve before and after the partial demagnetization. The model was also used to study the design of a special type of switched reluctance motor by Kim et al. (2005).

The demagnetization model of the Korean researchers (Kang, Kim, and Lee) was compared with a simple reluctance network based model by Kim et al. (2009). Their

simple reluctance models can analyze only the average flux density inside the magnets, like the first model of Farooq et al. (2006). The conclusion of the study was that the simple model should be used only as an initial design step.

2.4.7 Demagnetization by an Inclined Field

Sintered NdFeB magnets are anisotropic by nature. One grain of material can be magnetized only in one direction. The anisotropy is produced in the manufacturing process by aligning the grains in the magnetic field during the pressing. The degree of alignment of the grains affects the remanence, as described by Rodewald et al. (2000). The orientation degree is usually around 90-98%, depending on the manufacturing method. The orientation degree can be measured by a method described by Fernengel et al. (1996).

In demagnetization calculations, usually only the field component anti-parallel to the magnetic polarization is taken into account. This approximation leads to $1/\cos(\varphi)$ dependence of the demagnetization as a function of the angle φ between the magnetization and the demagnetizing field. In reality, the field component perpendicular to the magnetic polarization must also be taken into account, as shown by Elbaz et al. (1991) and by Givord et al. (1988). The dependence of the intrinsic coercivity on the angle φ lags behind the $1/\cos(\varphi)$ behavior in the case of large angles. In the papers of Martinek and Kronemüller (1990) and Gao et al. (2001) it is shown that the angular dependency of the intrinsic coercivity is also a function of the grain orientation. With a better grain orientation the behavior is closer to the $1/\cos(\varphi)$ behavior.

Katter (2005) studied the angular dependence of the demagnetization stability from the application point of view. He took into account the orientation degree of the magnets by comparing different manufacturing methods. He also presented a curve showing the demagnetization resistance as a function of the angle between the demagnetizing field and the magnetization direction. The curve was presented only for a few values of the angle.

Gutt and Lust (1990) studied the demagnetization of two-component ferrite magnets as a function of the angle between the demagnetizing field and the magnetization direction in a DC motor. They noticed that the component anti-parallel to the magnetization direction also has to be considered in modeling.

2.4.8   Magnetic Viscosity

A permanent magnet will slowly lose its magnetization because of thermal relaxation processes. This phenomenon is called magnetic viscosity. The phenomenon is well explained by Skomski and Coey (1999). The reduction of magnetic polarization J as a function of time t because of the magnetic viscosity obeys the logarithmic law

$$J_t = J_0 - S \log (t/t_0), \tag{2.3}$$

where S is the magnetic viscosity constant. According to Wohlfarth et al. (1984), the magnetic viscosity constant S depends on the temperature, the opposing magnetic field, the magnet material, and the magnetic history of the sample.

There are many publications by material scientists concerning magnetic viscosity. The viscosity behavior of sintered NdFeB magnets has been measured by Jubb and McCurrie (1987). Givord et al. (1987) studied the magnetic viscosity of NdFeB samples manufactured with different methods to study coercivity mechanisms. Within their research Givord et al. (1988) measured the magnetic viscosity constants as a function of the initial magnetizing field. The recent research into the phenomenon by Haavisto and Paju (2009) was conducted from the application point of view. They measured the loss of magnetization of NdFeB samples as a function of time using different NdFeB material grades, different temperatures, and different working points of the samples.

Electric machines with NdFeB magnets usually have quite a high working point. The magnets are normally not used near the knee region of the BH curve for a long time.

Thus, the loss of magnetic polarization because of magnetic viscosity is expected to be low. According to the figures in Haavisto (2009), the loss of magnetic polarization resulting from the magnetic viscosity in an electric machine will be negligible during a lifetime of 30 years. Thus, it is not necessary to take the magnetic viscosity into account in demagnetization modeling.

2.4.9 Mixed-Grade Design

If a permanent magnet machine is demagnetized, the magnets are not demagnetized uniformly. The surface magnets are, for example, demagnetized first from their edges. This observation gives rise to the idea of using multiple magnet grades in a single pole: in the areas which are more prone to demagnetization a material with higher intrinsic coercivity can be used. In other areas, a material with higher remanence can be used. This idea is called a mixed-grade design in this research.

Odor and Mohr (1977) introduced a mixed-grade idea for ferrite-based DC motors as early as in the 'seventies. In their idea, the trailing edge of the ferrite magnet in a DC motor has a higher intrinsic coercivity and smaller remanence than the leading edge of the magnet. They called these magnets "two-component magnets". The idea was patented by Robert Bosch GmbH. Later Gutt and Lust (1990) studied the demagnetization of this kind of ferrite arrangement and also took the inclined field into account.

The mixed-grade idea has also been used in scientific equipment. Thuillier et al. (2004) described a hexapole magnet for scientific equipment, where the radial field is generated by permanent magnets and the axial field by superconducting coils. The permanent magnet hexapole was divided in the radial and axial directions into sectors, where different magnet grades were used to maximize the remanence and also to secure the necessary intrinsic coercivity. The effect of the anti-parallel demagnetizing field caused by the superconducting coil was not considered.

2.4.10 Dovetail Machine

Buried magnet machines usually use several magnets to form one pole. This makes it easy to apply the mixed-grade design in buried magnet machines. Buried magnet machines can have a larger torque than surface magnet machines with the same rotor volume (Heikkilä, 2002). A drawback of buried magnet machines is the larger stray flux because of the iron bridges around the magnets. A special type of buried magnet machine geometry, namely a dovetail machine, patented by Kolehmainen (2008), was selected to study demagnetization and mixed-grade design. In the dovetail machine all the mechanical loads are carried by the magnets (Kolehmainen, 2007) and not by the small iron bridges, as in traditional buried magnet machines. The removal of these iron bridges also reduces the stray flux. Kolehmainen and Ikäheimo (2008) showed that a dovetail machine can have higher mechanical stability than traditional buried magnet machines, while the electrical properties and the use of the magnet material remain at the same level. Kolehmainen (2008, 2010) also studied dovetail machines with different pole numbers, showing that with low pole numbers, dovetail machines create a higher air-gap flux density, and with high pole number they can withstand a high rotational speeds.

2.4.11 Thermal Modeling with Parametric Models

The magnetic properties of permanent magnet materials are temperature-dependent. Thus, the demagnetization resistance of the material is also temperature-dependent. This means that it is important to include a thermal model in proper demagnetization modeling.

Parametric models have been widely applied for modeling the thermal behavior because of their flexibility. Perez and Kassakian developed a steady-state heat transfer model to calculate the temperatures in the different parts of a machine. The model is based on the thermal resistances between different parts of the motor. All three means of heat transfer are considered: conduction, convection and radiation. First, they used their model in an

optimization process of high-speed synchronous machines (1978). Later, they published a full paper that dealt with their thermal model only (1979). Their paper is one of the first comprehensive presentations of heat transfer modeling with a parametric model.

Parametric models can also include thermal capacitances in order to study the time-dependent thermal behavior. Mellor et al. (1991) built a model using linear differential equations and a lumped parameter network to study both steady-state and transient cases. Their model is formed completely using dimensions and physical constants, without any experimental data. The results were compared with measurements. They showed that their model can accurately predict the temperatures in different parts of the machine being studied. Thus, their publication clearly showed that it is possible to model the complex thermal behavior of an electric machine with a simple model.

In a machine, there can be a significant temperature difference in the axial direction. Kaltenbacher and Saari (1992) studied the thermal modeling of an enclosed induction machine using a parametric model. In their study they pointed out that the axial temperature differences can be modeled if the different cooling conditions of the different parts of the machine along the axial length are taken into account. They suggested a division of the machine frame into three parts: the drive end, non-drive end, and middle part. Rilla et al. (2008) measured temperatures inside a 60-kW, 9000-rpm machine. Their results also showed that large axial differences in temperature distribution can exist.

According to Jokinen and Saari (1997), the heating of the coolant can be an important source of losses in an electric machine. They calculated a coolant flow through a machine with a static parametric model. In their model, the coolant is treated with heat flow-controlled temperature sources. They also compared their calculation results with measurements. An important result of their study is that the heating of the coolant is more important in high-speed machines, where the heating of the coolant should be taken into account in thermal modeling. They also used a standard 15-kW induction machine as an example. In this machine, the heating of the coolant could be ignored. In

his licentiate (1995) and doctoral theses (1998) Saari developed a thermal analysis tool for high-speed induction machines. He concentrated on friction and gas flow losses. The model was used to estimate the maximum power of the machines at different rotating speeds. Finally, the model was evaluated against the test results of a real machine. The model that was developed was a detailed steady-state one based on a thermal resistance network.

A parametric thermal network can give accurate results if it is detailed enough. Rilla (2006) studied the thermal modeling of a permanent magnet machine in his master's thesis. He built a lumped parameter model with a very tight network, which makes it possible to see, for example, the temperature distribution inside a stator slot quite clearly. The model was tested by calculating the temperature distribution of three permanent magnet machines and by comparing the results with measurements.

2.4.12   Thermal Modeling with FEM

The thermal modeling of an electric machine requires a 3D model. 3D FEM models are heavy in calculations and slow to build. This is one reason why parametric models have been in use for a long time. Negrea and Rosu (2001) compared a surface magnet machine and a permanent magnet machine with pole shoes. They performed the electromagnetic analysis with a 2D FEM tool and the thermal analysis with a 3D simulation package. The thermal calculations were not compared against any measurements. Their study showed that the rotor losses of the surface magnet machine are larger, and they concluded that because of the larger rotor losses and because of the configuration, the surface magnet machine is more prone to magnet demagnetization.

Negrea et al. (2001) modeled temperatures inside a large permanent magnet machine with pole shoes using a 3D thermal analysis tool. The results were compared with the measurements. The 3D calculation proved to be too slow for transient analysis, and thus they built a lumped parameter model for it. The lumped parameter model was used to study different short circuit cases. It was noted that a one-phase short circuit causes the

highest rise in temperature, while a three-phase short circuit is the least dangerous. Thus, it was suggested that the frequency converter should connect all the phases together to form a three-phase short-circuit if a one- or two-phase short circuit is detected in order to reduce the damage.

2.4.13   Eddy Current Modeling

To calculate the temperatures correctly with the thermal model, all sources of thermal energy, or losses, must be calculated accurately. The eddy currents are an important source of losses in electric machines. Especially in a permanent magnet machine rotor losses, eddy currents in permanent magnets play an important part. According to Maxwell's equations, eddy currents flow in a plane perpendicular to the varying component of magnetic flux density. Thus the eddy current phenomenon is three-dimensional in its nature.

Normally, 2D FE modeling is used for the electromagnetic calculations of electric machines. In these 2D calculations, eddy current losses cannot be accurately calculated, unless some correction factors are used, which take into account the change of geometry from 3D to 2D.

Eddy current losses are normally modeled using Maxwell's equations with a quasistatic approximation, where the displacement currents are ignored. Schmidt et al. (2008) studied the modeling error caused by this approximation. Their paper showed that the error might be important if the piece being modeled is larger than the inducing wavelength, or if the piece being modeled has low conductivity or high permittivity, and if the inducing frequency is high.

Many analytical models have been developed to calculate the eddy current losses. Markovic and Perriard (2007, 2008) introduced an analytical method that can be applied to cylindrical rotor geometry with a slotless stator. The method is quite complex, with modified Bessel functions, and it can be used only, if the stator is not saturated. Polinder

and Hoeijimakers (1997) derived an analytical equation to calculate the eddy current loss density in permanent magnets in a long 2D geometry. They verified their model by locked rotor tests. Later Polinder and Hoeijimakers (1999) used the model to estimate the eddy current losses of an inverter-driven machine. On the basis of the model that was derived they showed the effect of magnet segmentation in a circumferential direction to reduce the losses. Zhu et al. (2004) published an improved analytical model for the eddy current calculations of brushless surface magnet machines. Their model was based on a large number of earlier models and it takes into account both time and space harmonics. The model is two-dimensional, and thus it does not take into account the end-effects and the magnet length. The effect of slotting was also neglected.

2.4.14   Magnet Segmentation

Atallah et al. (2000) developed an analytical model to estimate the rotor losses of brushless machines where the fundamental stator MMF has fewer poles than the rotor and the rotor is thus running on a harmonic wave. In their publication they also studied the effect of the circumferential segmentation of the permanent magnets. They suggested using two to four segments, as it is both practical and effective. Toda et al. (2004) used the model to compare the eddy current losses on the rotor side. They compared a tooth-coil wound machine and a traditionally wound machine. In both cases, they showed that the circumferential slotting of the magnets is important from the loss reduction point of view. Ishak et al. (2005) extended the model further in their study of the eddy current losses in different fractional slot winding configurations. They also compared the losses in cases, where the motor is used either in a synchronous mode or in a brushless DC mode. They pointed out that the brushless DC mode causes more eddy current losses on the rotor. Their model was two-dimensional and thus did not take the magnet length into account.

Ede et al. (2007) studied the effect of both the circumferential and the axial segmentation of the permanent magnets in the reduction of rotor losses. A new model was developed in which the eddy current distribution inside the magnets is modeled in

three dimensions, while the machine in general is modeled in two dimensions. Their paper showed that the axial segmentation is also a very important method in the reduction of the eddy currents, in contrast to an earlier publication by Kirtley et al. (1998). According to Kirtley et al., the axial segmentation should not have an important effect on the reduction of the eddy currents.

Wu et al. (2002) modeled an outer rotor PM generator with FEM. They studied the effect of magnet slicing and rotor back-iron lamination into the rotor eddy current losses. They divided the rotor eddy current losses on back-iron eddy current losses and magnet eddy current losses. In their geometry, it was noticed that if laminated back-iron is used instead of solid back-iron, the total eddy current losses in the rotor might even increase.

Jussila (2009) designed an axial-flux machine with fractional-slot winding in her dissertation. The magnets in the rotor were tested in three different configurations: magnets sliced in a tangential direction, magnets sliced in a radial direction, and bulky magnets. In the design, the bulky magnets could not be used at all because of high eddy current losses. The losses of the two sliced solutions were about the same, showing that the direction of the slicing did not have an effect in the machine that was studied.

2.4.15 Resistivity of NdFeB Material

One way to take into account the third dimension in the 2D calculation of eddy currents is to adjust the resistivity of the permanent magnets. Kesavamurthy and Rajagopalan presented a method to take into account the end-effects of the rotor by adjusting the resistivity of the rotor as early as in 1959. Their correction was based on empirical equations. There were several equations, one for each type of induction machine in their publication.

Russell and Norsworthy (1958) studied the end-effects of induction machines. Their end-effect formulation, or the Russell-Norsworthy end-coefficient, was used by Deak et

al. (2008) to adjust the resistivity of the magnet material to study eddy current losses. Another method to adjust the resistivity of the magnet material to correct the end-effects was presented by Binder et al. (2004). The correction was used again in a publication by Deak et al. (2006).

The electrical resistivity of permanent magnet materials can be found in the datasheets of the magnet manufacturers (Vacuumschmelze, 2008) or in the standard IEC 60404-8-1 (2004). A major drawback in these values is that the temperature dependence or the anisotropy of resistivity is not reported. Thus, many publications concerning eddy current losses have been made by using a room temperature value of the resistivity.

The electrical resistivity of NdFeB permanent magnet material was studied by material scientists in the 'eighties and in the 'nineties. The studies show the temperature dependence of the materials, but the results are used to detect phase transitions or other matters important for material scientists: the resistivity itself, which is important for electrical engineers, was not focused on in the research. No study of the resistivity of the latest commercial rare earth magnet materials is available.

Jen and Yao (1987) studied the resistivity of two NdFeB alloy compositions. The resistivity as a function of temperature was published, but unfortunately the alloys that were used were chemically quite far from the alloys used in the twenty-first century. Later, Yao et al. (1988) published the temperature dependence of the resistivity of the same alloys between 4 K and 1200 K. The same research group (Wu et al., 1997) later studied the temperature dependence of the resistivity of thin films and compared the results to the resistivity of the bulk material. The same compositions were used.

Gutfleisch et al. (1993) used resistivity measurements as a tool for metallurgic research. They studied, for instance, phase transitions and magnetic transitions as a function of temperature by measuring the resistivity (Gutfleisch et al. 1993). In their paper, Gutfleisch et al. (1993) noticed that the resistivity of rare earth magnets is anisotropic in its nature.

2.4.16   Conclusion of Literature Study

There have been many publications involving the modeling of demagnetization. Demagnetization has been modeled in different situations and using different models, but there have not been any publications about the demagnetization model itself. The earlier models in publications assume a *BH* curve consisting of two lines: the roundness around the knee-point of the *BH* curve is not taken into account. The earlier models also ignore the demagnetizing field perpendicular to the magnetizing direction. Only in some publications is it mentioned that the perpendicular field must also be considered when studying the demagnetization of NdFeB magnets.

The dynamics of the demagnetization phenomenon have not been studied. It is very important to know how the demagnetization will affect the behavior of the machine, including the thermal behavior. In earlier studies the demagnetization and the thermal behavior were not studied together.

The resistivity of rare earth magnets has been measured and also shown to be anisotropic by material scientists. The anisotropy of the resistivity can have significant consequences for the eddy current calculations. The electrical engineers would also need to know the resistivity of the magnet material as a function of temperature. Previous eddy current calculations in earlier publications were carried out without considering anisotropy or the temperature dependence of the resistivity, because practical data about resistivity of this kind were not available for electrical engineering purposes.

Eddy current calculation has been the subject of a huge number of publications. In earlier publications, most eddy current calculations were made with analytical methods or 2D FE modeling, because the more accurate 3D FE modeling is too time-consuming. Some authors have presented methods to take into account the finite length of the permanent magnets in 2D FE simulations by adjusting the resistivity of the magnet material. However, the accuracy of these methods has not been reported.

A traditional permanent magnet machine is built using only one magnet grade. There have been some publications where, especially, ferrite motors have been built using several magnets with different magnetic properties. Because of the price difference between the NdFeB magnet grades, the use of several magnet grades in NdFeB permanent magnet machine can offer cost benefits, in addition to the technical benefits. The commercial issues of a machine with several magnet grades have not been discussed.

This research is expected to develop a good tool to model the demagnetization of NdFeB magnets in permanent magnet machines. The approach is to include thermal calculations and to improve the accuracy of the simulation of the eddy current losses in permanent magnets. A mixed-grade pole will be used as an example in the calculations and testing.

3   The Tool for Demagnetization Modeling

The tool built during this study consists of several models: an FEM model, a demagnetization model, an eddy current model, and a thermal model. The existing 2D FE software developed by Helsinki University of Technology was used as a platform for the other models. The demagnetization model and the eddy current model were implemented in the code of the FE software. The thermal model was implemented as a separate entity. The models are described in more detail later in this chapter.

3.1   FEM Model

The demagnetization model and the eddy current model were implemented in the existing 2D FEM model. The FE software has been developed at Helsinki University of Technology since the 'eighties. The FEM model uses the Crank-Nicolson scheme-based time-stepping method. The iterative solver uses the Newton-Raphson algorithm. The permanent magnets are treated as solid conductive bars in the model. An integrodifferential formulation is used to ensure that no induced net current flows from one magnet to another. A detailed description of the FE software is given by Arkkio (1987).

3.2   Demagnetization Model

The demagnetization model is the main outcome of this research. It communicates directly with the FEM model. The demagnetization model checks each element containing permanent magnet material for demagnetization after each time-step. If any demagnetization occurs, the demagnetization model updates the magnetic polarization of the elements and the time-step is recalculated.
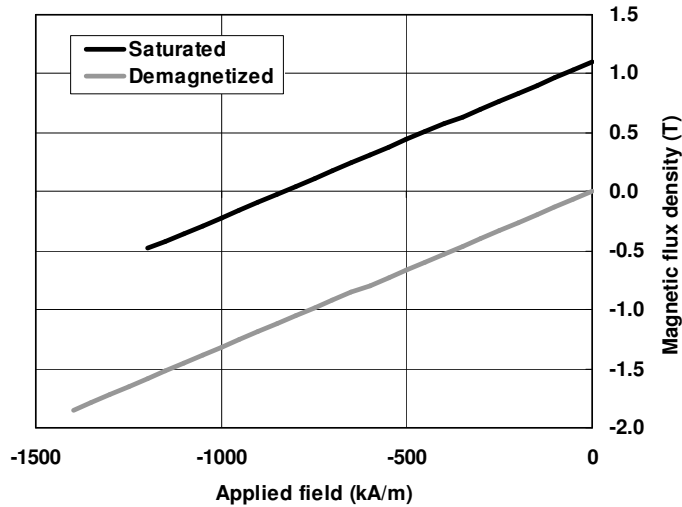
Fig. 3.1 The coercivity limit model.

The demagnetization model uses one of four different *BH* curve models, which are shown in Figures 3.1, 3.2, 3.3, and 3.4. The simplest model, the coercivity limit model, is presented in Fig 3.1. In this model, the *BH* curve is a straight line up to a certain limit, which is usually the intrinsic coercivity $_jH_c$. If the working point goes beyond the limit during a time-step, the magnetic polarization of the element is set to zero and the time-step is recalculated.

The next models, the vertical coercivity model and the two-piece linear model, can be seen in Figures 3.2 and 3.3 respectively. These models were used in the publications by the Korean research group (Kang, Kim, and Lee), which was mentioned in the literature study. In these models the *BH* curve is formed of two lines. If the working point at any time-step goes on a vertical or on a steeply falling line in any element inside a permanent magnet material, the magnetic polarization in that element is updated and the time-step is recalculated. In the vertical coercivity model the vertical part of the *BH*

66

curve is at the intrinsic coercivity. In the two-piece linear model, the slope of the second part of the curve can be adjusted. The two-piece linear model can simulate the real behavior of permanent magnets quite accurately, as was shown in P1.

The real *BH* curves of magnetic materials always have some roundness around the knee-point. The last model (presented in Fig 3.4), the exponential model, takes this into account. The details of the exponential model are given in the next subchapter.
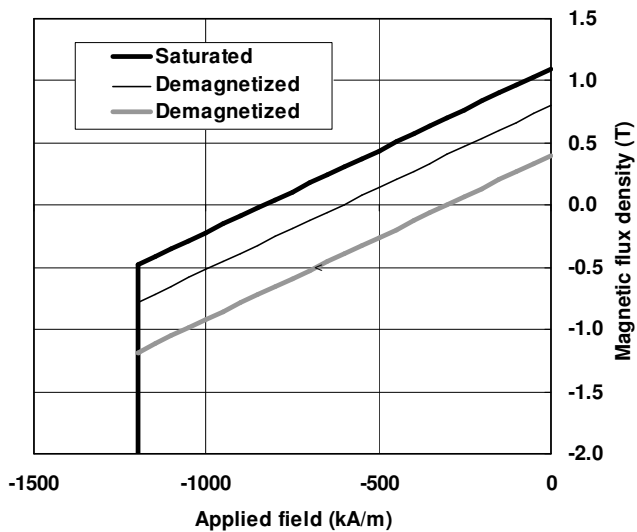
Fig. 3.2 The vertical coercivity model. The *BH* curve is formed of two parts. The vertical part is located at the intrinsic coercivity $_JH_c$.
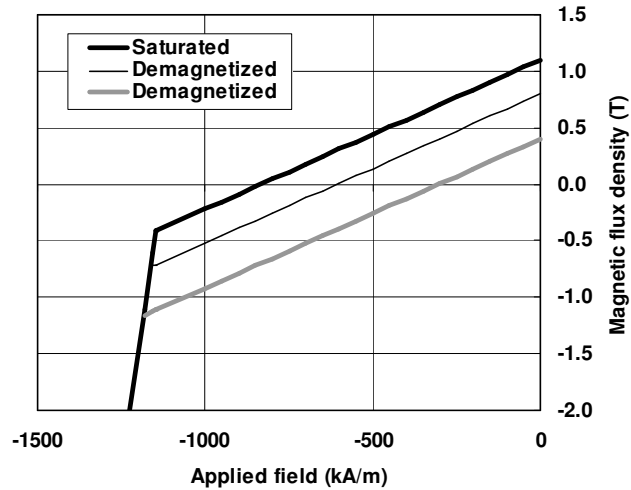
Fig. 3.3 The two-piece linear model. The *BH* curve is modeled with the lines. The slope of the steeply falling part of the *BH* curve can be adjusted.

The FEM model performs the calculations using a linear *BH* curve. After each time-step, the working point of each element is checked using one of the four demagnetization models described. If the working point falls beyond the knee-point of the *BH* curve, the magnetic polarization of that element is updated, as shown in Fig 3.4. After that, the time-step is recalculated. Normally, some five iterations are needed for one time-step when demagnetization happens.
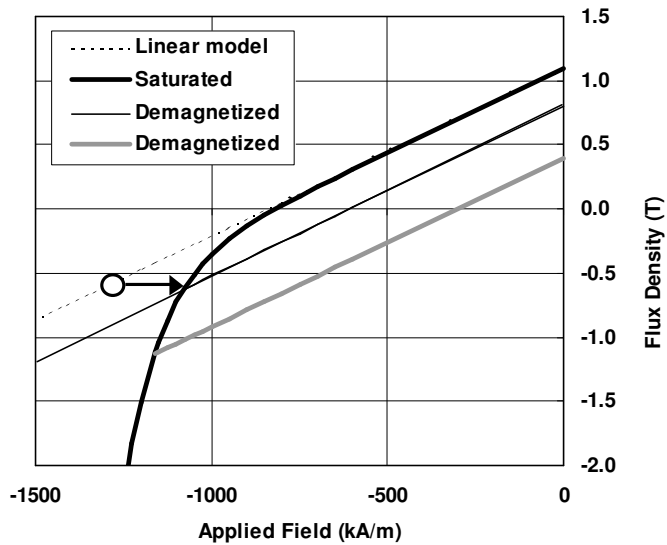
Fig. 3.4 The exponential model. The roundness of the *BH* curve can be adjusted. If the working point (a circle in the figure) goes too far on the negative *H*-axis, the working point is returned to the *BH* curve by dropping the magnetic polarization.

3.2.1 Squareness

The most important properties of the permanent magnet material are: the remanence B_r, intrinsic coercivity $_JH_c$, the slope of the *BH* curve (μ_r) and the squareness of the curve. The exponential model of the *BH* curve was developed to be able to take the squareness of the curve into account. In this model, the *BH* curve is given by the following function:

$$B = B_r + \mu_0 \mu_r \cdot H - E \cdot e^{K_1 \cdot (K_2 + H)}, \tag{3.1}$$

where E is a constant needed for unit conversion. E = 1 T. The input values are B_r, $_JH_c$, μ_r, and K_1. The parameter K_1 defines the squareness of the curve as shown in Fig 3.5. the parameter K_2 is calculated with the following equation:

$$K_2 = \frac{\ln\left[(B_r + (\mu_r - 1) \cdot \mu_0 \cdot {}_JH_c) \cdot \dfrac{1}{E}\right]}{K_1} - {}_JH_c \; . \tag{3.2}$$

With this model, a good agreement with the measured hysteresis curves and calculated *BH* curves can be achieved if K_1 has a value around $-6 \cdot 10^{-5}$ m/A.
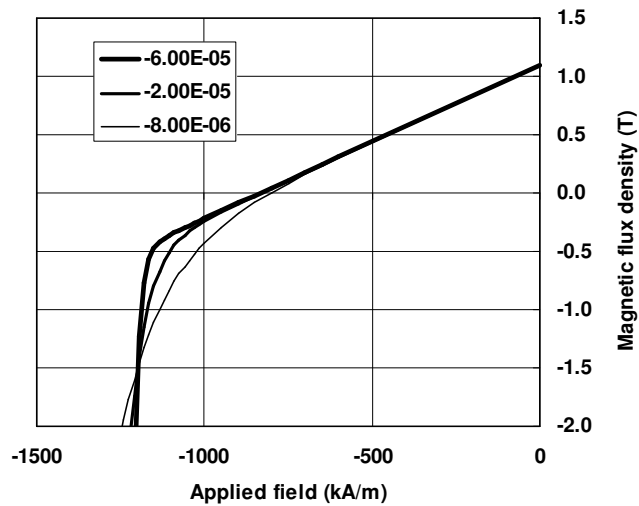
Fig. 3.5 The effect of the parameter K_1 on the squareness of the curve.

70

3.2.2   Temperature Dependence

The magnetic properties are temperature-dependent. The temperature dependence of the intrinsic coercivity is approximately linear over the normal usage temperatures of permanent magnet applications. The temperature dependence of remanence is slightly different: it follows a downwards-sloping parabola. However, in the normal temperature range of the electric machines, the linear approximation is still satisfactory. Fig 3.6 shows the measured temperature dependence of remanence and intrinsic coercivity. In the model, the remanence and intrinsic coercivity are defined at two temperatures for each magnet grade. A linear interpolation is used to estimate the values between these temperatures.
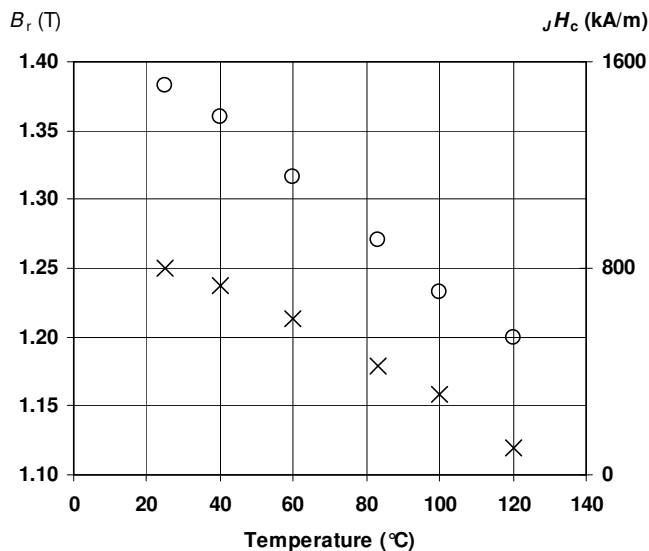
Fig. 3.6 Remanence (crosses) and intrinsic coercivity (circles) of an NdFeB magnet sample as a function of temperature. Both quantities have approximately linear behavior as a function of temperature over the presented temperature range.

3.2.3 Demagnetization by an Inclined Field

In demagnetization calculations, only the demagnetizing field component anti-parallel
to the direction of magnetic polarization is usually taken into account. Katter (2005) has
shown that the field component perpendicular to the direction of magnetic polarization
must also be taken into account. It was decided to include the effect of the inclined
demagnetizing field in the model. Numerous pulse demagnetization measurements were
made with samples manufactured with several magnet grades, as described in P4. The
demagnetization as a function of the pulse field strength was plotted for each angle and
each grade. The field strength $H_{k, 90\%, \varphi}$, where the magnet was 10% demagnetized, was
defined as a function of the inclination angle φ. When $H_{k, 90\%}$ was divided by $H_{k, 90\%}$
value at zero inclination, $H_{k, 90\%, 0}$, the curves of different grades showed similar
behavior, as shown in Fig 3.7. This means that it is possible to describe the effect of the
inclined field on demagnetization with a simple function.

It was decided to include the effect of the inclined field in the model accordingly: the
intrinsic coercivity calculated at a certain temperature is modified according to the
following equation acquired by a curve fitting to the results in Fig 3.7:

$$_J H_c^{ANG} = {_J}H_c \left(1 + a_1 \varphi + a_2 \varphi^2 + a_3 \varphi^3 \right), \tag{3.3}$$

where $a_1 = +3.17 \cdot 10^{-4}$ deg^{-1}, $a_2 = -3.38 \cdot 10^{-5}$ deg^{-2}, and $a_3 = +1.37 \cdot 10^{-6}$ deg^{-3}. The
modified intrinsic coercivity is then used in the demagnetization model instead of the
original value.
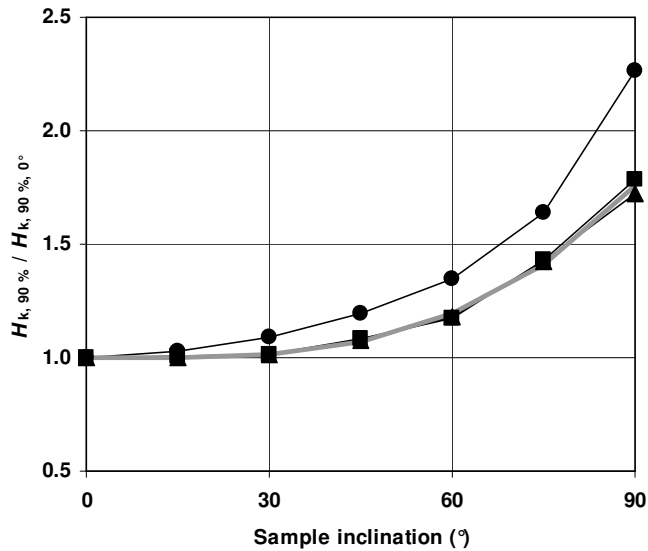
Fig. 3.7 Relative field strength required to demagnetize the sample by 10 % compared to the field strength at zero inclination as a function of the inclination angle. Three samples with intrinsic coercivities 1050 kA/m (circles), 1635 kA/m (triangles), and 2080 kA/m (rectangles) were used. The gray line is the line drawn by function (3.3).

3.2.4   Recoil Curve

The coercivity of sintered NdFeB material is based on nucleation. As stated before, the minor loops of the materials with nucleation as their coercivity mechanism show minor loops with a very small surface area (Phelps and Atherton, 2001). Figures 3.8 and 3.9 show the minor loops of the sintered NdFeB magnets measured for this research. It can be seen that if the vertical axis is not crossed, the minor loop does not have a detectable surface area.

An interesting feature in Figures 3.8 and 3.9 is that the recoil curve bends upwards near the vertical *B*-axis. This non-linearity would need to be modeled if it were significant. However, as stated in P3, the recoil curve can be modeled with a straight line if the demagnetization is small. The recoil curves are treated as straight lines in this model.
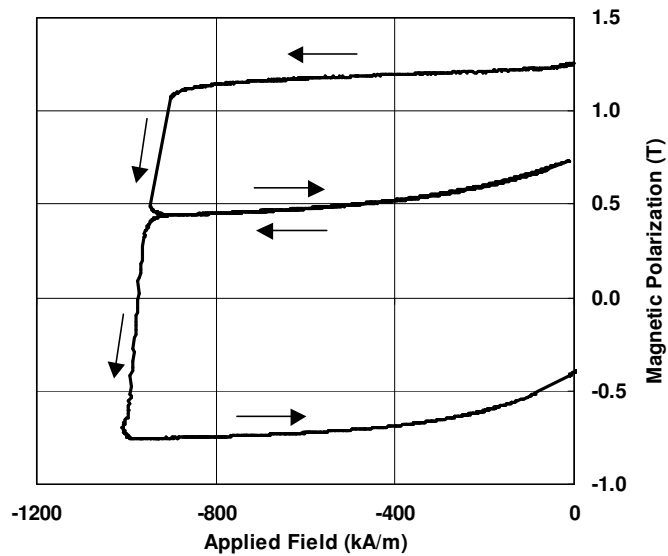
Fig. 3.8 A recoil curve of a sintered NdFeB magnet. The recoil curve can be seen bending upwards near the vertical *B*-axis.
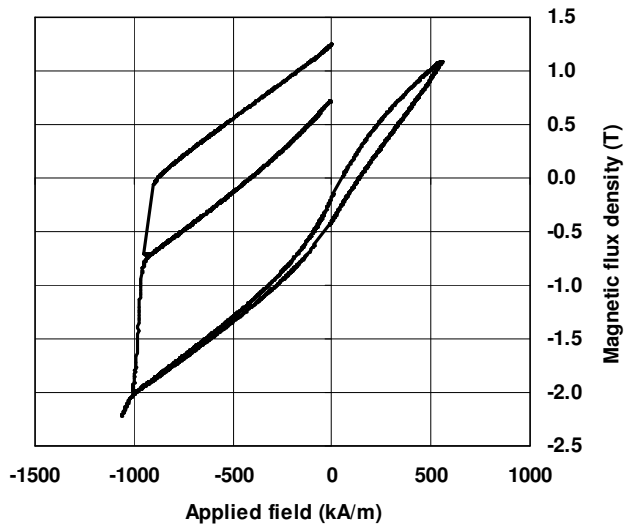
Fig. 3.9 A recoil curve of a sintered NdFeB magnet crossing the *B*-axis. A minor loop with a significant surface area is formed only if the vertical axis is crossed.

3.3   Thermal Model

A thermal model was needed in the tool to take into account the temperature dependence of the magnetic properties and the resistivity. The parametric thermal model was selected over a thermal FEM model because of its simplicity. The parametric model can also be adapted more easily to different machines. It was decided to use as simple a parametric model as possible to make the adaptation to different machines as easy as possible. The model can be adjusted to simulate the thermal behavior of an electric machine by adjusting the three thermal resistances. The thermal model used in this research is presented in Fig 3.10.

Because the magnetic properties and the resistivity of the conductor material and the permanent magnet material are temperature-dependent, the information needed from the

model was the magnet temperature and the stator conductor temperature. The total losses, divided into rotor losses, stator resistive losses and iron losses are used as input variables, in addition to the ambient temperature.

Even with large losses, it takes some time to heat up the machine. On the other hand, the electrical phenomena take place during a few electric cycles. Thus, the time constant in the thermal calculations is a lot larger than in the electromagnetic calculations. For this reason, the thermal model is separated from the other models. It was also decided to restrict the study to the steady-state phenomena, and thus, the thermal capacitances were excluded from the thermal model.

Fig.3.10 A schematic presentation of the simple parametric thermal model for calculating the temperatures in the nodes (T_{rotor}, T_{Fe}, T_{stator}) with three sources of heat ($P_{rotor}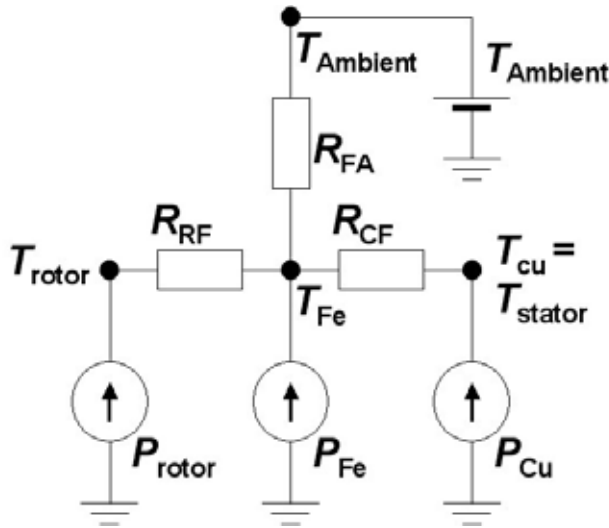$, P_{Fe}, P_{Cu}), three thermal resistances (R_{RF}, R_{FA}, R_{CF}) and a given ambient temperature ($T_{Ambient}$).

3.4   Eddy Current Model

The eddy current model was included in the tool to improve the calculation accuracy of the eddy current losses in permanent magnets. A good accuracy of eddy current losses is needed to get correct results from the thermal model.

In a 2D FE analysis, a cross-section of the machine is modeled. If the machine is long, the end-effects will not cause a large error in the calculations. However, this does not apply to permanent magnets: for practical manufacturing reasons, the length of the permanent magnet is limited to around 100 mm. A rotor of a modern permanent magnet machine can be more than 1000 mm in length. So there can be several magnets, which are not connected to each other electrically, making the eddy currents flow in each magnet separately. The eddy currents in the adjacent ends of magnets cancel each other approximately from the magnetic field solution point of view making the problem more suitable for 2D calculations, as shown in Fig 3.11. However, the eddy currents in the magnet ends still cause losses and have an effect on the magnitude of the axial eddy currents, which means that they must be taken into account somehow even in 2D modeling.

In previous publications, resistivity values between 1.4 μΩm and 1.6 μΩm for the resistivity of NdFeB magnets were used. These values can be found in standards and in the data sheets of the manufacturers. Because the NdFeB material is anisotropic, the resistivity is different in different directions. The data sheet values of resistivity have been measured in the magnetization direction, i.e., in the direction where the eddy currents normally do not flow. The value of resistivity perpendicular to the magnetization direction is much smaller, causing a systematic error in all previous eddy current calculations. It is also important for the electrical engineer to know the resistivity of the permanent magnet material at different temperatures. Previously, no practical data have been available about the temperature dependence of the resistivity of permanent magnets.
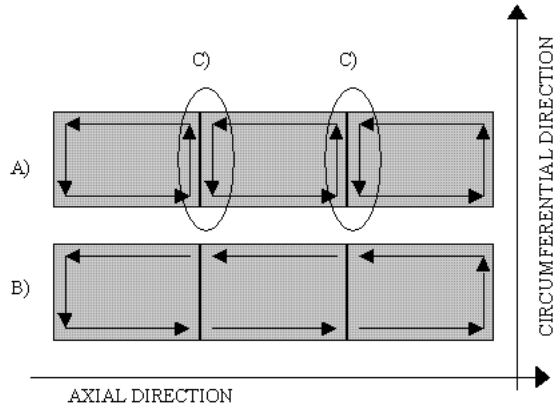
Fig. 3.11 Eddy currents in a row of magnets (A) in a radial flux machine. The eddy currents in the magnet ends (C) cancel each other from the magnetic field solution point of view making 2D approximation reasonable (B). However, the currents still cause losses in the magnet ends (C), which is ignored in 2D calculations.

3.4.1 Resistivity as a Function of Temperature

The resistivity of the rare earth magnets was measured in P5. Both magnetized and unmagnetized samples were used. The resistivity was measured in the orientation direction and perpendicular to the orientation direction. Different NdFeB magnet grades were used. The measurements were performed over the temperature range -40 ℃… +150 ℃, which is typical for modern permanent magnet machines. It was noticed that all the magnet grades measured had the same resistivity within the measurement accuracy. The magnetization of the sample did not have an effect. There was a significant difference between the resistivity in the orientation direction and perpendicular to the orientation direction. The resistivity results of the measurements for sintered NdFeB material can be found in Fig 3.12.

78

The resistivity value perpendicular to the orientation direction is more important in the eddy current calculations, since the eddy currents mostly flow perpendicular to the orientation direction. The value of resistivity is taken into account in the eddy current model with the following linear curve fitting:

$$\rho(\mu\Omega m) = 0.92 \cdot T \ (^\circ C) + 1.25, \tag{3.4}$$

which gives the value of the resistivity perpendicular to the orientation direction as a function of temperature.

3.4.2 Anisotropic Resistivity

The resistivity was found to be anisotropic in P5. The difference between the resistivity value in the orientation direction and perpendicular to the orientation direction was found to be approximately 18% at room temperature. To find out if anisotropic resistivity should be used in accurate eddy current calculations, a series of simulations, published in P7, was performed. The same machine was modeled by 2D FEM, by 3D FEM using isotropic resistivity, and by 3D FEM using anisotropic resistivity. In the 3D isotropic case, the resistivity value used was the resistivity perpendicular to the orientation direction. In all cases, the resistivity value at 80°C was used.
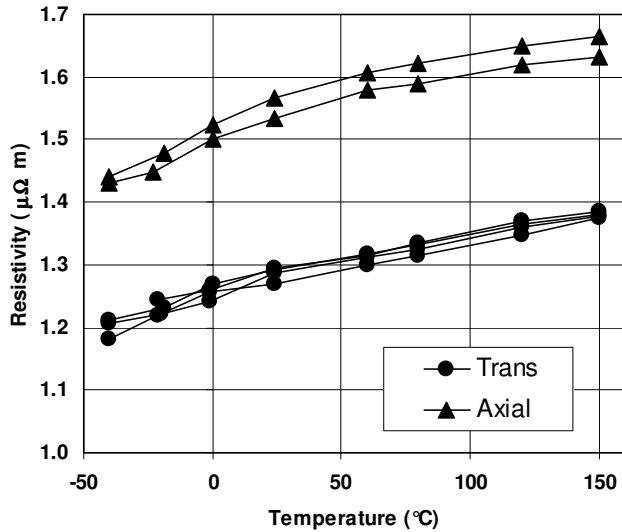
Fig. 3.12 The resistivity of sintered NdFeB magnet material as a function of temperature. The resistivity in the orientation direction (axial) is a lot greater than the resistivity perpendicular to the orientation direction (trans).

The results of the calculations can be seen in Fig 3.13. It can be seen that the 2D calculation gives losses that are too large. On the other hand, both 3D cases have almost the same results, meaning that a single-valued resistivity can be used in eddy current calculations instead of the physically more realistic anisotropic resistivity, as long as the resistivity value perpendicular to the orientation direction is used. In 2D FE simulations, where the eddy currents can flow only parallel to the symmetry axis, the resistivity perpendicular to the orientation direction must be used.
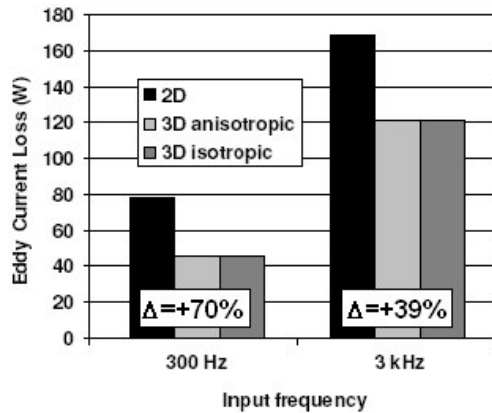
Fig. 3.13 Eddy current losses in the permanent magnets of a surface magnet machine calculated with three different methods: 2D, 3D with anisotropic resistivity and 3D with isotropic resistivity. The losses were calculated using different input frequencies. Losses calculated with the 2D method are too large, while both 3D methods give the same results.

3.4.3 Third Dimension in 2D Eddy Current Calculations

To improve the eddy current calculation accuracy in 2D FE modeling, it was decided to study if the resistivity could be adjusted according to the magnet shape. Three analytical equations were derived to calculate the eddy current losses in a block magnet. In each equation, the eddy currents were assumed to follow a different path, as shown in Fig 3.14. The models based on the analytical equations are called Model A, Model B and Model C. The models are based on the following assumptions:

- The magnetic flux density is uniform throughout a magnet.
- The problem is resistance limited, i.e., the frequency is relatively low.
- The eddy current flows in one plane, i.e., the eddy-current density is the same through the thickness.

The equations of the Models A, B and C can be found in P6.
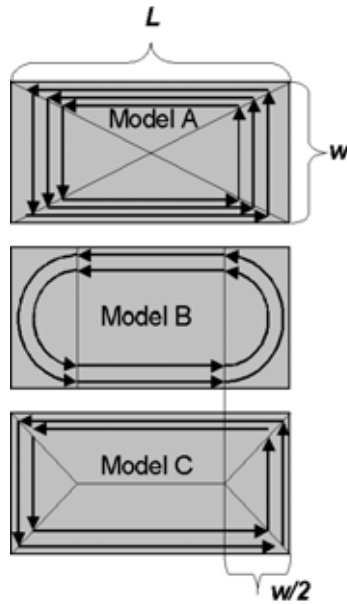
Fig. 3.14 The eddy current paths in analytical calculations. An equation for the eddy current losses was derived in each case above.

Another method was also tried to improve the calculation accuracy of the eddy current losses. The eddy currents of three different block magnets were modeled both with 2D FEM and with 3D FEM. With 3D FEM the magnet length was varied. The calculation method is described in P6. The 2D and the 3D results were compared. If the ratio of the losses was plotted as a function of K

$$K = \frac{hL}{w},\tag{3.5}$$

where w is the magnet width (mm), h is the magnet thickness (mm), and L is the magnet length (mm), the curves showed similar behavior, as shown in Fig 3.15. A function that was as simple as possible was searched for to follow the behavior of the calculation results. As a result, a function which is called model X was found. The function gives

the relative difference between the 2D and 3D eddy current calculation results as follows:

$$\frac{P_{3D}}{P_{2D}} = 1 - C_2 \frac{w}{hL} = 1 - C_2 \frac{1}{K}, \tag{3.6}$$

where C_2 = constant: 3 mm. This function is presented in Fig 3.15. In Fig 3.16 the analytical models A, B, and C, some calculation results, and model X can be seen together for comparison.
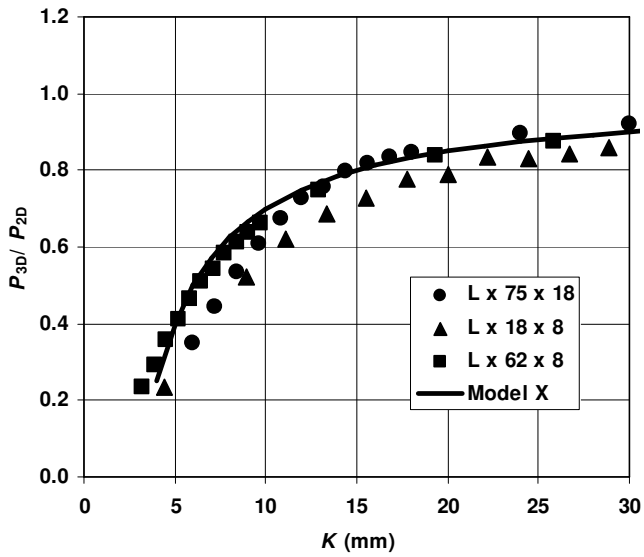
Fig. 3.15 Relative difference in eddy current calculation results as a function of K. In addition to the calculation results, model X is also presented. The calculation results were acquired by modeling the eddy current losses of three different block magnets in 3D and in 2D and by varying the magnet length. K is a function of magnet dimensions (3.5).
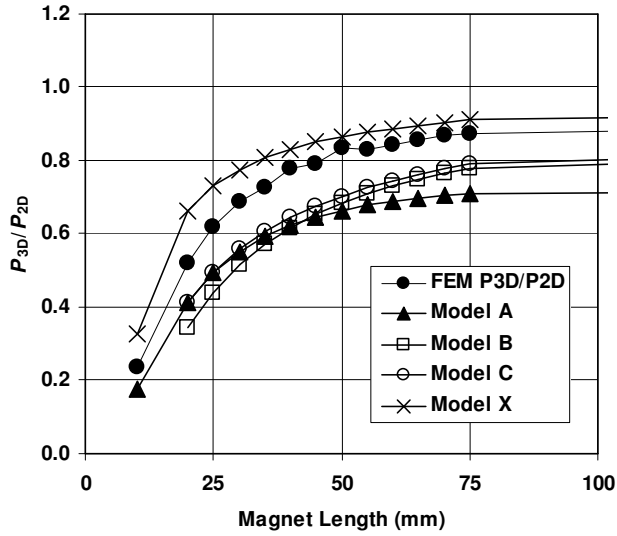
Fig. 3.16 Relative difference in eddy current losses in 2D and 3D simulations as a function of the magnet length. The results of the analytical models A, B, and C are presented together with the results of the model X and the simulation results.

The relative difference in eddy current losses in 2D and 3D calculations can be given by the factor F

$$F = \frac{P_{3D}}{P_{2D}}. \tag{3.7}$$

F can be calculated according to model A as follows:

$$F = \frac{P_{3D}}{P_{2D}} = \frac{3}{4} \cdot \frac{L^2}{w^2 + L^2}. \tag{3.8}$$

F can be calculated according to model X as shown in (3.6).

If the low-frequency eddy currents are the most significant in the problem, the problem is called resistance-limited. In that case the resistivity can be adjusted directly with the factor F.

In the eddy current model of this research, the resistivity is adjusted both as a function of temperature and as a function of the magnet shape. Both model A (3.8) and model X (3.6) can be used. The resistivity is then given with the following function:

$$\rho = \frac{b \cdot T + a}{F} ,$$
(3.10)

where the coefficients a and b are according to Equation (3.4).

Models A and C were compared in P6 by modeling a surface magnet machine both in two and three dimensions. The 2D calculations were made with model A, with model X and without correction. The results of the calculations are presented in Table I.

The results show that the calculation accuracy of the eddy currents is improved after the correction. If the 3D calculation result is assumed to be a correct value, there is still a difference after the corrections, but the accuracy is a lot better.

TABLE I
EDDY CURRENT LOSS IN PERMANENT MAGNETS

Case	Input: 300 Hz, 92 A	Input: 3 kHz, 9.2 A
3D (ρ=1.32 $\mu\Omega$m)	45.49 W	121.31 W
2D (ρ=1.32 $\mu\Omega$m) (difference to 3D)	77.9 W (+71%)	168.4 W (+39%)
Corrected: model A 2D (ρ=2.13 $\mu\Omega$m) (difference to 3D)	51.1 W (+12%)	110.5 W (-8.9%)
Corrected: model X 2D (ρ=1.89 $\mu\Omega$m) (difference to 3D)	57.1 W (+26%)	123.3 W (+1.6%)

3.5   The Dataflow of the Tool

The models exchange data with each other (Fig 3.17). During every time-step, the FEM model solves the magnetic flux density in each element of the permanent magnet. The demagnetization model then checks if any demagnetization happens in any element. In the case of demagnetization, the magnetizations of the demagnetized elements is given as a new input values to the FEM model and the time-step is recalculated. If there is no demagnetization, the next time-step is solved. If the time-step was the last one, the simulation is ended and the loss powers are printed to output data.

The thermal model uses the loss powers in the output data to calculate the temperatures in different parts of the machine. The magnetic properties and the resistivity of the permanent magnet material are temperature-dependent. The temperatures of the stator conductors and permanent magnets are given as input parameters to other models. The demagnetization model adjusts the magnetic properties of the magnet grades according to the magnet temperature. The eddy current model adjusts the resistivity of the permanent magnet material according to the magnet temperature. The FEM model adjusts the conductivity of the conductors according to the stator temperature. The data link between the thermal model and the other models is handled manually by the user.

The eddy current model is used to adjust the resistivity of the magnet material according to the magnet temperature and the magnet shape. The eddy current model is only used to set up the initial values.
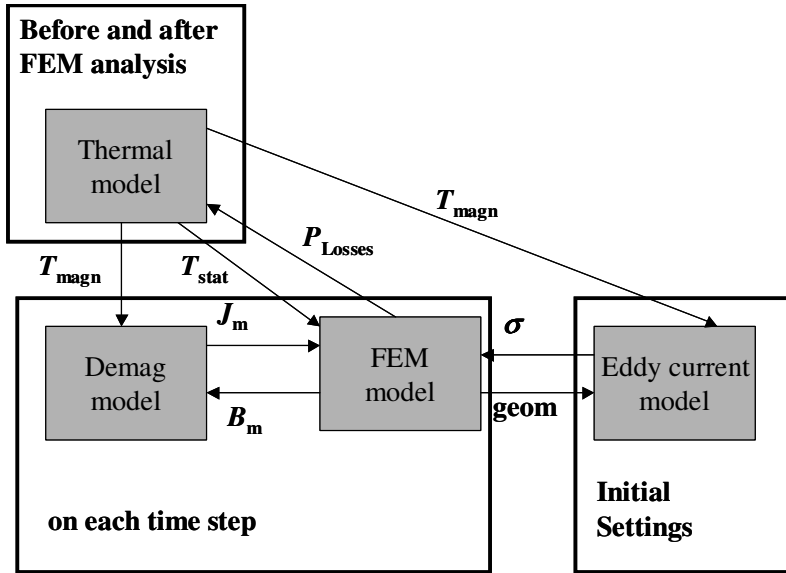
Fig. 3.17 The dataflow between the models of the tool.

4 Demagnetization Model Evaluation

The demagnetization model was tested by comparing the results with a real demagnetization of the magnets after a locked-rotor experiment on an overheated machine. Different magnet grade combinations were used in the poles of the machine during the tests. In this chapter, the demagnetization tests are described. How the demagnetization should be modeled in different situations is also studied.

4.1 Mixed-Grade Pole

Traditionally, only one permanent magnet material grade has been used in permanent magnet machines. The grade is selected to be such that it creates a large enough magnetic flux and can also withstand all operating conditions without a significant risk of demagnetization. However, not all parts of the pole in a permanent magnet machine are stressed in the same way: in a surface magnet motor, for example, the trailing edge of the magnet is most prone to demagnetization in overloading. In a buried magnet machine, the parts of the magnets which are closest to the surface of the rotor are most prone to demagnetization in the event of a short circuit.

As mentioned before, NdFeB magnets can be manufactured in several grades. Some grades have higher remanence but relatively low intrinsic coercivity, while some grades have lower remanence but high intrinsic coercivity. The grades with high intrinsic coercivity are more expensive because of their chemical composition. If only one magnet grade is used, it must be selected to be able to resist demagnetization in the worst part of the pole. If several magnet grades can be used, a high-coercivity material can be selected for the worst parts of the pole and a higher-remanence material for the other parts. As a result, the pole will still be able to resist demagnetization, but creates a higher flux. The main idea of this "mixed-grade pole" is that the magnetic properties of the magnets in a pole can be different in different parts of the pole.

The mixed-grade pole has several benefits. As mentioned before, the pole is magnetically better, because it can resist the same demagnetizing conditions while creating a higher flux. The cost of the magnet material in the pole will decrease, because some of the high-coercivity material is replaced by a material with higher remanence. As shown in Fig 2.2, material with higher remanence has less dysprosium. Since dysprosium is more expensive than neodymium, the pole will be cheaper. The reduction in the consumption of dysprosium is also good from the point of view of the usage of natural resources, because in rare earth ores there is usually a lot more neodymium than dysprosium.

In large machines, a pole is usually constructed of several magnets. In these cases the use of a mixed-grade pole is easy, because individual magnets of different grades can be selected. For example, a machine type suitable for mixed-grade construction is a dovetail machine, shown in Fig 4.1.

The mixed-grade structure in a six-pole salient pole machine was studied in P2 by modeling the demagnetization of the machine after a three-phase short circuit. A single-grade structure which can survive the fault shows a lower EMF than the mixed-grade structure which is able to survive a fault. Thus it was shown that in the modeled six-pole machine the use of the mixed-grade structure would be beneficial.
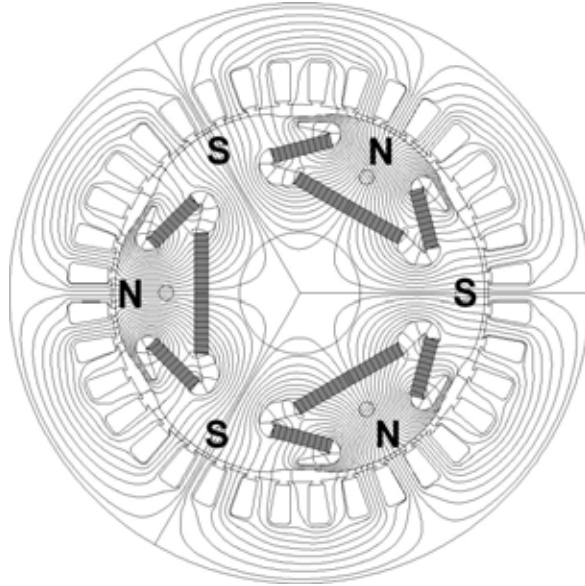
Fig. 4.1 A cross-section of a six-pole dovetail machine. There are magnets only on every other pole. The poles with the magnets are constructed of an iron core and three magnets. In a dovetail machine, the magnets carry the centrifugal stresses.

4.2   Comparison with Measurements

The demagnetization model was tested by modeling a locked-rotor situation at an elevated temperature with sinusoidal input, and comparing the results with real in situ tests. The selected machine was the dovetail machine shown in Fig 4.1. The simulations were performed at different temperatures and with different input current values. It was noticed that the temperature must be measured very accurately in the tests to get comparable results. Small changes in the input current value did not have such a large effect on the demagnetization. It was also noticed that the demagnetization in the left-hand, right-hand and middle magnets is a function of the position to which the rotor is locked, as can be seen in Fig 4.2. The calculations and the tests are described in greater detail in P8.
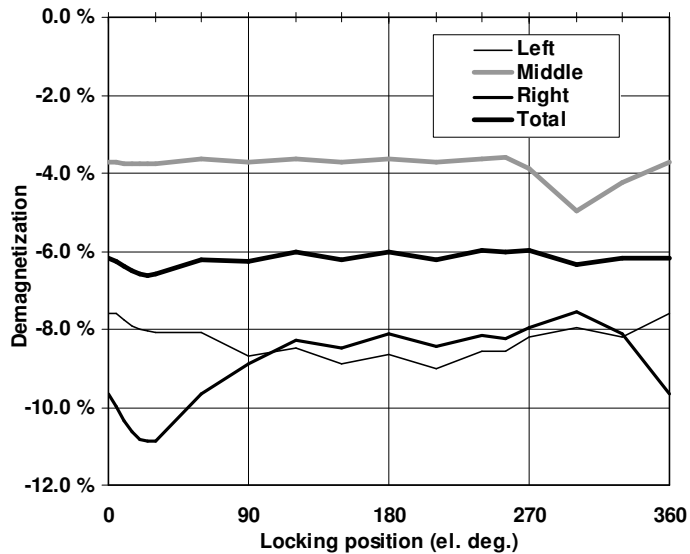
Fig. 4.2 Calculated demagnetization of the simulated single-grade pole after a locked-rotor situation with a sinusoidal 100-Hz current of 165 A fed to the stator. The demagnetization of different magnets is a function of the locking position.

Two different magnet configurations were tested. In the first one, all the magnets were of the same grade. In the second test, the middle magnet was replaced with a material with lower intrinsic coercivity but with higher remanence. The temperatures for the locked-rotor tests were selected to cause approximately 5% demagnetization.

The test results of the single-grade pole are presented in Fig 4.3. The experimental results show similar behavior to the calculations. The difference in the magnitude of the demagnetization can be explained by the fact that the demagnetization is a sensitive function of the testing temperature. The difference in the demagnetization between the left-hand, right-hand and middle magnets can be explained by the different locking angles (Fig 4.2). The rotor position during the test was not measured.
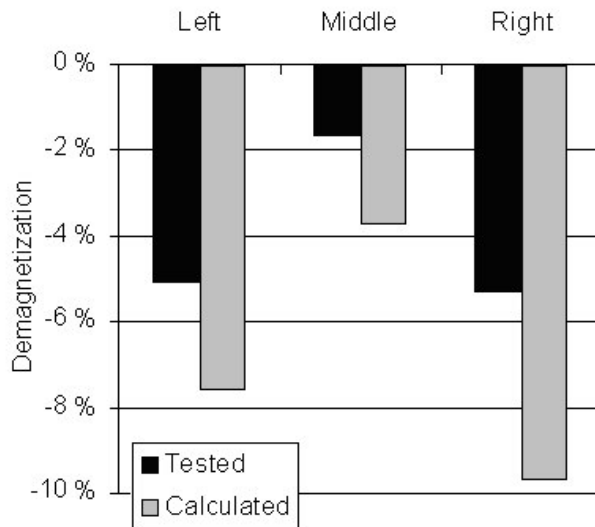
Fig. 4.3 Measured demagnetization of the magnets of a dovetail machine compared with the calculated demagnetization. The tested case is a locked-rotor situation at 180 °C when the stator was fed with a 100-Hz sinusoidal current of 165 A. Only one magnet grade is used.

In the first test with the single-grade pole, the middle magnet has the lowest demagnetization. For the second test, the middle magnet was replaced by a magnet with higher remanence but less intrinsic coercivity, because the middle magnet was found to be less prone to demagnetization according to the first test. The test results of the mixed-grade pole are shown in Fig 4.4. The test results are similar to the calculation results. Now the middle magnet is demagnetized more than the side magnets.

After the tests, it can be concluded that the demagnetization model can estimate the demagnetization of a real electric machine accurately. The test reported in P8 was the first test where a demagnetization model was evaluated against a real in situ testing.
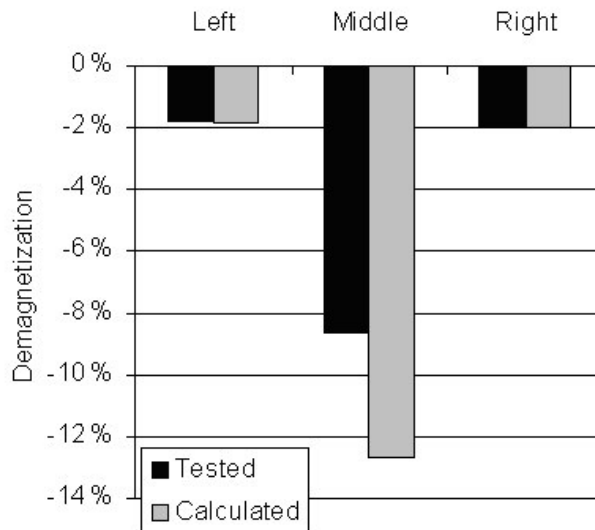
Fig. 4.4 Measured demagnetization of the magnets of a dovetail machine compared with the calculated demagnetization. The tested case is a locked-rotor situation at 175 °C when the stator was fed with a 100-Hz sinusoidal current of 165 A. The magnets in the middle have higher remanence and lower intrinsic coercivity than the magnets on the sides.

4.3 The Dynamics of the Demagnetization

When demagnetization is being modeled, the whole dynamics of the system must be considered. The loading of the machine, the moment of inertia of the system, and the thermal characteristics of the system must be taken into account.

The demagnetization can happen rapidly as a result of a transient or during a constant overloading or because of an elevated temperature. If the demagnetization occurs because of a short circuit, the operation of the machine is usually stopped. Thus, to model a short circuit, a short simulation can be enough, because everything happens in the matter of a couple of electric cycles. However, if the machine is loaded with a

93

constant torque and it becomes demagnetized by overloading or by too high a temperature, the situation is different. The machine will compensate for the demagnetization by increasing its load angle. This will increase stator currents, which will instantly cause more demagnetization. After a while, the losses caused by the increased temperatures will cause even more demagnetization. If the machine is still loaded with a constant torque, this process can go on and on according to Fig 4.5 until the machine stalls.

The demagnetization of a machine loaded with a constant torque was studied using simulations in P9. A thermal model of the machine was formed. The machine was overheated in the simulations by increasing the ambient temperature.

The first simulations in P9 were carried out without the thermal model. The machine was simulated for two electric cycles with a fixed load angle. If there was demagnetization after the simulation, the load angle was corrected to maintain the same torque. The iteration of the load angle was repeated until there was no more demagnetization. The second simulations were also performed without the thermal model. These simulations were very long simulations, lasting around 10 hours each. The machine was loaded with a constant torque, and the load angle could change to adjust to the loading. The test was repeated with different values of the moment of inertia.

When the first and the second simulations are compared, the results are the same: the demagnetization caused a slight increase in the load angle, after which the demagnetization did not grow any more. These tests show that the demagnetization caused by heating with a constant torque can be accurately calculated with a series of short tests instead of a single long test.

```
          ┌──────────────────────┐
     ┌───▶│   DEMAGNETIZATION    │
     │     └──────────┬───────────┘
     │                │
     │                ▼
     │     ┌──────────────────────┐
     │     │     CHANGE OF        │◀──┐
     │     │     LOAD ANGLE       │──┐│
     │     └──────────┬───────────┘  ││
     │                │              ││
     │                ▼              ││
     │     ┌──────────────────────┐  ││
     │◀────│   MORE CURRENT       │◀─┘│
     │     │   => MORE LOSSES     │   │
     │     └──────────┬───────────┘   │
     │                │               │
     │                ▼               │
     │     ┌──────────────────────┐   │
     │     │     CHANGE OF        │   │
     │     │    TEMPERATURE       │   │
     │     └──────────┬───────────┘   │
     │                │               │
     │                ▼               │
     │     ┌──────────────────────┐   │
     │◀────│     CHANGE OF:       │───┘
           │  RESISTANCE AND      │
           │     REMANENCE        │
           └──────────────────────┘
```
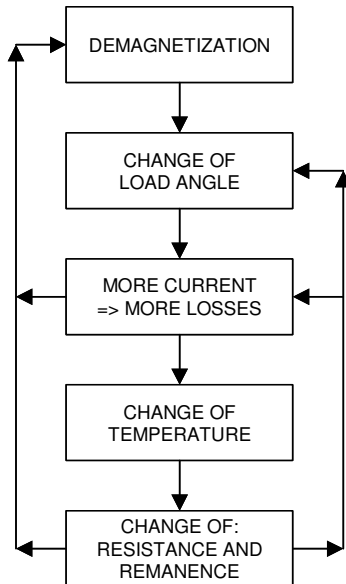
Fig. 4.5 The dynamics of the demagnetization of a permanent magnet machine loaded with a constant torque.

The third set of simulations was performed with the thermal model. The demagnetization was first calculated in a similar way as in the first tests. After there was no more demagnetization resulting from the change in the load angle, the temperature was calculated again according to the new losses. Then the load angle iteration was repeated. After some iteration of temperature and load angle, it was noticed that the machine was heating up until it stalled. Only if the initial demagnetization was very small did the increase in the temperature not lead to stalling. The simulations in P9 show clearly that the thermal properties of the machine must be included in the demagnetization calculations.

5   Discussion

A model to simulate the demagnetization of a permanent magnet was developed in this research. The new model is based on the exponent function and it is easy to use and can be defined with only four parameters. The model can take into account the roundness around the knee of the *BH* curve. The new model was compared with linear models found in earlier publications in P1. The new model also takes into account the demagnetizing field component perpendicular to the orientation direction. In earlier publications, this component was usually considered not to have any effect. The importance of the perpendicular field component was shown in P4. In the model, the magnetic properties are temperature-dependent. The recoil curve of the model is straight. It was shown in P3 that the recoil curve actually bends upwards near the *B*-axis. The recoil curve did not show a significant loop. The effects of magnetic viscosity were not taken into account in the model.

The new model was evaluated in P8 by comparing the simulation results and experimental results. The results proved that the model could be used to simulate demagnetization. No such comparison had been reported before in the literature.

Parts of the tests in P8 were performed using a special mixed-grade pole machine presented in P2. In the mixed-grade pole machine, there can be several magnet grades in one pole. A similar idea was presented for ferrite magnets in the 'seventies. When a mixed-grade pole with NdFeB magnets is applied, there can be both technical and commercial benefits.

The dynamics of the demagnetization were considered in P9. A study was made of how the demagnetization should be simulated. A machine loaded with a constant torque and demagnetized in operation by increased temperature was used as an example. How the demagnetization drifts further because of heating until the machine stalls was shown. According to the simulations in P9, it was shown that it is important to include a

thermal model in demagnetization modeling. The demagnetization result must be iterated together with temperature. There was no publication about the demagnetization modeling itself before P9.

The resistivity of the rare earth magnets was measured in P5 as a function of temperature. It was noticed that the resistivity is different in the orientation direction and perpendicular to it. The resistivity value given in standards is the value in the orientation direction. However, the eddy currents usually flow perpendicular to the orientation direction in permanent magnet machines. The resistivity value perpendicular to the orientation direction is smaller than in the orientation direction. Since most of the earlier eddy current modeling was performed using the table value, there is a systematic error in most eddy current calculations. The resistivity was given in P5 as a function of temperature, both in the orientation direction and perpendicular to it. The values were given for $SmCo_5$, Sm_2Co_{17}, and NdFeB magnets. These resistivity values were measured in the 'eighties by the material scientists, but there were no practical data on modern materials available for electrical engineers.

As the resistivity was found to be anisotropic, there was a need to check if the eddy current calculations should be performed using anisotropic resistivity. A surface magnet machine was modeled in P7 both in 3D and 2D. The 3D modeling was performed both with an isotropic resistivity value and with anisotropic resistivity. The results showed that the difference between the isotropic and anisotropic 3D calculations was insignificant. Thus, the isotropic value should be used, because with the scalar resistivity the calculations are faster. However, it should be noted that the resistivity value measured perpendicular to the orientation direction should be used. It was also noticed in P7 that the difference in results between the 2D and 3D calculations was significant.

Publication P6 was written to reduce the calculation error in 2D eddy current calculations. The idea was to adjust the resistivity according to the shape of the magnet. This idea has also been used before in the literature. However, in P6 the method

97

according to which the adjustment is made is new. First, three analytical equations were derived for eddy current power in a block magnet. After that, the eddy currents of three different block magnets were simulated in a sinusoidal magnetic field. The magnet length was varied. A curve was fitted to these results. It was shown that the analytical equations, the curve-fitting model, and the simulations show similar behavior. The new models were tested by simulating the eddy currents of a permanent magnet machine in 3D and in 2D. The 2D modeling was performed with and without the correction by adjusting the resistivity. The 3D results were assumed to be correct. It was shown that the accuracy of the eddy current calculation could be improved by the resistivity correction that was introduced.

5.1   Future Work

The recoil behavior of NdFeB magnets could be measured with higher accuracy. It was shown in P3 that the recoil curves could be modeled using third-order polynomials. If curved recoil curves are included in the demagnetization model, it can have an effect on the stability of the FEM model.

The resistivity of rare earth magnets was measured between –40 °C and +150 °C. It could be interesting to expand the measuring range, especially towards the higher temperatures, since many machines can now run even at 200 °C. Because the resistivity is anisotropic, it is natural to assume that the thermal conductivity would also be anisotropic. The thermal conductivity should also be measured in two directions.

The eddy current models are under constant development. In some years, 3D calculations will be fast enough to be used in standard machine design. However, 2D modeling will still be used after that, because a 2D model is easier to construct. Thus, it is important to keep on pursuing higher eddy current calculation accuracy in 2D too.

5.2 Summary

The goal of this work has been to improve the modeling of irreversible permanent magnet demagnetization in the FE analysis of electric machines. A demagnetization model with new features was created. With the new model it is possible to simulate the behavior of an electric machine after a fault where the machine gets demagnetized. It is also possible to study what happens during the demagnetization.

A mixed-grade pole idea was introduced. In a mixed-grade pole, the use of two or more magnet grades in a pole results in improved performance but also has the potential to reduce the cost of the NdFeB magnet material. A machine with a mixed-grade pole was used in real in situ testing of the demagnetization model.

The eddy current calculation accuracy was improved by introducing resistivity values of the magnet material as a function of temperature. A shape-based correction for 2D FE analysis was also introduced.

The dynamics of demagnetization were considered. It was shown that in demagnetization modeling, the dynamics of the whole system have to be considered. A thermal model must be included and the final state of demagnetization can be calculated in an iterative manner.

References

Allcock, R. 2009. Sales Manager, Vector Fields Software, Cobham Technical Services, United Kingdom. Personal communication, 2009. roger.allcock@cobham.com, www.cobham.com

Arkkio, A. 1987. "Analysis of induction motors based on the numerical solution of the magnetic field and circuit equations", Diss., Helsinki University of Technology, Acta Polytechnica Scandinavica, no. 59.

Arshad, W. M., Chin, Y. K., Bäckström, T., Soulard, J., Östlund, S., Sadarangani, C. 2001. "On Finding Compact motor Solutions for Transient Applications", Electric Machines and Drives Conference, Cambridge, MA, USA, pp. 743-747.

Asianmetal, June 2010, available online: http://www.asianmetal.com/.

Atallah, K., Howe, D., Mellor, P., Stone. D. 2000. "Rotor Loss in Permanent-Magnet Brushless AC Machines", IEEE Transactions on Industry Applications, vol. 36, No. 6, pp. 1612-1618, Nov/Dec 2000.

Binder, A., Klohr, M., Schneider, T. 2004. "Losses in high speed permanent magnet motor with magnetic levitation for 40000/min, 40 kW," in Proc. ICEM'04, Cracow, Poland, September 2004, CD-ROM, 6 p.

Boucherit, A., Srairi, S., Djerdir, A., Miraoui, A. 2004. "Analytical and Numerical Modelling of Demagnetization Phenomenon in a Permanent Magnet Motor", in Proc. ICEM'04, Cracow, Poland, September 2004, vol. 1, pp. 127-128.

Campbell, P. 1994. "Permanent Magnet Materials and their Application", Cambridge University Press.

Deak, C., Petrovic, L., Binder, A., Mirzaei, M., Irimie, D., Funieru, B. 2008. "Calculation of eddy current losses in permanent magnets of synchronous machines," in Int. Symp. Power Electronics, Electrical Drives, Automation and Motion, Jun. 11–13, 2008, pp. 26-31.

Deak, C., Binder, A., and Magyari, K. 2006. "Magnet loss analysis of permanent-magnet synchronous motors with concentrated windings," in Proc. ICEM, 2006, p. 6, CD-ROM.

Dorrell, D.G., Klauz, M. 2003. "Design improvements in a permanent-magnet commutator machine including the use of rare earth magnets", IEMDC'03: Electric Machines and Drives Conference, June 2003, pp 166-172 vol. 1.

Ede, J., Atallah, K., Howe, D. 2007. "Effect of Axial Segmentation of Permanent Magnets on Rotor Loss in Modular Permanent-Magnet Brushless Machines", IEEE Transactions on Industry Applications, vol. 43, No. 5, pp. 1207-1213, September/October 2007.

Elbaz, D., Givord, D., Hirosawa, S., Missel, F. P., Rossignol, M. F. and Villas-Boas, V. 1991. "Angular dependence of coercivity in sintered RFeB magnets", J. Appl. Phys., vol. 69, pp. 5492-5494.

Enokizono, M., Kumoi, M., Kawano, S. 1994. "Finite Element Analysis of Anisotropic Magnetic Materials Taking Rotation Magnetization into Account", IEEE Trans. Magn., vol. 30, no. 5, pp. 3387-3390, September 1994.

Enokizono, M.,Matsumura, K., Mohri, F. 1997. "Magnetic Field Analysis of Anisotropic Permanent Magnet Problems by Finite Element Method", IEEE Trans. Magn., vol. 33, No 2., pp. 1612-1615, March 1997.

Enokizono, M., Takahashi, S., Kiyohara, T. 2003. "Magnetic Field Analysis of Permanent Magnet Motor with Magnetoanisotropic Materials Nd-Fe-B", IEEE Trans. Magn., vol. 39, No 3, pp 1373-1376, May 2003.

Farooq, J. Srairi, S., Djerdir, A., and Miraoui, A., 2006a. "Use of permeance network method in the demagnetization phenomenon modeling in a permanent magnet motor," IEEE Trans. Magn., vol. 42, no. 4, pp. 1295-1298, Apr. 2006.

Farooq, J., Djerdir, A., and Miraoui, A. 2006b. "An Inverse Problem Methodology to Analyze Demagnetization Phenomenon in Permanent Magnet Machines", 12th Biennial IEEE Conference on Electromagnetic Field Computation, 2006, conference proceedings, p. 41.

Fernengel, W., Lehnert, A., Katter, M., Rodewald, W. and Wall, B. 1996. "Examination of the degree of alignment in sintered Nd–Fe–B magnets by measurements of the remanent polarizations," J. Magn. Magn. Mat., vol. 157, pp. 19-20.

Gao, R. W., Zhang, D. H., Zhang, Y. M., Li, W., Wang, Y. S. and Yu, X. J. 2001. "Effect of the intergrain interactions on the coercivity and its angular dependence for Nd(FeCo)B sintered magnets," J. Magn. Magn. Mat., vol. 224, pp. 125-131.

Givord, D., Heiden, C., Hoöhler, A., Tenaud, P., Viadieu, T., Zeibig, K. 1988. "Dependence of the Coercive Field and Magnetic Viscosity Coefficient in NdFeB Magnets on the Magnetic History of the Sample", IEEE Trans. Magn., vol. 24, No. 2, pp 1918-1920, March 1988.

Givord, D., Tenaud, P., Viadieu, T. 1988. "Angular dependence of coercivity in sintered magnets," J. Mag. Mag. Mat., vol. 72, pp. 247-252.

Givord, D., Tenaud, P., Viadieu, T. 1987. "Magnetic viscosity in different Nd-Fe-B magnets", J. Appl. Phys. 61 (8), pp 3454-3456, April 1987.

Goldenberg, C., Lebensztajn, L., Lobosco, O.S. 1997. "Analysis of short-circuit transients of a PM machine", Electric Machines and Drives Conference Record, Milwaukee, USA, May 1997, pp: WB2/13.1-WB2/13.3.

Grössinger, R., Harada, H., Keresztes, A., Kirchmayr, H.R., Tokunaga, M. 1987. "Anisotropy and hysteresis studies of highly substituted Nd-Fe-B based permanent magnets", IEEE Trans. Magn., vol. 23, No. 5, pp 2117-2119, September 1987.

Gutfleisch, O., Verdier, M., Harris, I. 1993. "Magnetic and phase transitions and HDDR process in NdFeB-type alloys monitored by electrical resistivity measurements", Journal of Alloys and Compounds, 196 (1993), L19-L21.

Gutfleisch, O., Verdier, M., Harris, I., Ray, A. 1993. "Characterisation of rare earth-transition metal alloys with resistivity measurements," IEEE Trans. Magn., vol. 29, no. 6, pp. 2872-2874, Nov. 1993.

Gutt, H.-J., Lust, R. 1990. "Numerical Field Calculation of Additional Non-Linear Effects and Additional Non-Linear Components in Permanent Excited Machines", IEEE Trans. Magn., vol. 26, No. 2, pp. 532-535, March 1990.

Haavisto, M., Paju, M. 2009. "Temperature Stability and Flux Losses Over Time in Sintered Nd-Fe-B Permanent Magnets", IEEE Trans. Magn., vol. 45, No. 12, pp 5277-5280, December 2009.

Harrison, R. 2009. "Physical Theory of Ferromagnetic First-Order Return Curves", IEEE Trans. Magn., vol. 45, No. 4, pp. 1922-1939, April 2009.

Heikkilä, T. 2002. "Permanent magnet synchronous motor for industrial inverter applications - analysis and design", Diss., Lappeenranta University of Technology, Acta Universitatis Lappeenrantaensis 134. Lappeenranta, Finland.

Hitachi Special Metals, 2007. "Sintered Nd-Fe-B Magnets: The Patent and License Situation", April 2007, available in: www.hitachi-metals.co.jp/e/.

IEC, 2004. "Specifications for Individual Materials—Magnetically Hard Materials", IEC standard: 60404-8-1, 2004, p. 65, IEC:2001+A1.

Ishak, D., Zhu, Z., Howe, D. 2005. "Eddy-Current Loss in the Rotor Magnets of Permanent-Magnet Brushless Machines Having a Fractional Number of Slots Per Pole", IEEE Trans. Magn., vol. 41, No. 9, pp. 2462-2469, September 2005.

Jen, S., Yao, Y. 1987. "Electrical resistivity and specific heat studies of Nd-Fe-B magnet around its Tc," J. Appl. Phys., vol. 61, no. 8, pp. 4252-4254.

Jiles, D. 1991. "Introduction to Magnetism and Magnetic Materials", London, UK, Chapman & Hall.

Jokinen, T., Saari, J. 1997. "Modelling of the coolant flow with heat flow controlled temperature sources in thermal networks", IEE Electric Power Applications, vol. 144, Issue: 5, pp: 338-342, ISSN 1350-2352, Sep. 1997.

Jubb, G. A., McCurrie, R. A. 1987. "Hysteresis and Magnetic Viscosity in Nd-Fe-B Permanent Magnet", IEEE Trans. Magn., vol. 23, No. 2, pp 1801-1805, March 1987.

Jussila, H. 2009. "Concentrated Winding Multiphase Permanent Magnet Machine Design and Electromagnetic Properties – Case Axial Flux Machine", Diss., Lappeenranta University of Technology, Acta Universitatis Lappeenrantaensis 374. Lappeenranta, Finland.

Kaltenbacher M., Saari J. 1992. "An asymmetric thermal model for totally enclosed fan cooled induction motors", Helsinki University of technology, Laboratory of Electromechanics, Report 38.

Kang Do Hyun, Curiac, P., Lee Ju 2000. "An Axial Flux Interior PM Synchronous Machine", in Proc. ICEM 2000, Espoo Finland, August 2000, pp. 1475-1479.

Kang, G.-H., Hur, J., Sung, H.-G., and Hong, J.-P. 2003a. "Optimal design of spoke type BLDC motor considering irreversible demagnetization of permanent magnet," in Proc. 6th Int. Conf. Electr. Machines Syst., Beijing, China, vol. 1, pp. 234-237.

Kang, G.-H., Hur, J., Nam, H, Hong, J.-P., and Kim, G.-T. 2003b. "Analysis of irreversible magnet demagnetization in line-start motors based on the finite-element method," IEEE Trans. Magn., vol. 39, no. 3, pp. 1488-1491, May 2003.

Katter, M. 2005. "Angular dependence of the demagnetization stability of sintered Nd–Fe–B magnets," IEEE Trans. Magn., vol. 41, no. 10, pp. 3853-3855, Oct. 2005.

Katter, M. 2005. "Angular dependence of the demagnetization stability of sintered Nd–Fe–B magnets," Intermag 2005, IEEE International Magnetics Conference, Nagoya, Japan, April 4.-8., 2005, Proceedings, page: 473.

Kennedy, D. 2009. "Rare Earth Permanent Magnet Raw Materials Supply", Magnews, Summer 2009, pp 32-33.

Kesavamutrhy, N., Rajagopalan, P. K. 1959. "The polyphase induction machine with solid iron rotor," Trans. AIEE, vol. 78, pp. 1092-1098.

Kim, T.H., Choi, S-K., Ree, C-L. and Lee, J. 2005. "Effect of Design Variables on Irreversible Permanent Magnet Demagnetization in Flux-Reversal Machine", Proceedings of the Eighth International Conference on Electrical Machines and Systems, ICEMS 2005, September 2005, vol. 1, pp. 258-260.

Kim, K.-C., Kim, K., Kim, H.J., Lee, J. 2009. "Demagnetization Analysis of Permanent Magnets According to Rotor Types of Interior Permanent Magnet Synchronous Motor", IEEE Trans. Magn., vol. 45, no 6, pp. 2799-2802, June 2009.

Kim, K.-C., Lim, S.-B., Koo, D.-H. and Lee, J. 2006. "The shape design of permanent magnet for permanent magnet synchronous motor considering partial demagnetization," IEEE Trans. Magn., vol. 42, no. 10, pp. 3485-3487, Oct. 2006.

Kirtley, J., Tolikas, M., Long, J., Ng, C., Roche, R. 1998. "Rotor loss models for high speed PM motor-generators," in Proc. ICEM, 1998, pp. 1832-1837.

Kobayashi, K., Akiya, T., Nakamura, M., Hayakawa, K., Sagawa, M. 2004. "Magnetic Reversal Mechanism of Saturable Multi-Domain Particles in Zn/Sm2Fe17N3 Reacted Powders," HPMA'04 – 18th International Workshop on High Performance Magnets and Their Applications, Annecy (France), 29 August – 2 September.

Kolehmainen, J. 2007. "Machine with a rotor structure supported only by buried magnets," in Int. Symp. Electromagnetic Fields, Prague, Sep. 2007, 6 pages.

Kolehmainen, J. 2008. "Rotor for a Permanent-Magnet Electrical Machine,", WO Patent 2008025873 (A1), Mar. 6, 2008.

Kolehmainen, J. 2008. "Dovetail permanent magnet rotor solutions with different pole numbers," in Proc. 2008 Int. Conf. Electrical Machines, in Proc. ICEM 2008, Paper ID 939, 4 pages.

Kolehmainen, J. 2010. "Optimal dovetail permanent magnet rotor solutions with various pole numbers," IEEE Transactions on Industrial Electronics, vol. 58, Issue: 1, pp. 70-77, Jan. 2010.

Kolehmainen J., Ikäheimo, J. 2008. "Motors with buried magnets for medium-speed applications," IEEE Trans. Energy Convers., vol. 23, no. 1, pp. 86-91, Mar. 2008.

Lampola, P. 1999. "Optimisation of low-speed permanent-magnet synchronous machines with different rotor designs", Electromotion, vol. 6, No. 4, pp: 147-159, October-December 1999.

Lampola, P., Saransaari, P. 2000. "Analysis of a Multipole, Low-Speed Permanent-Magnet Synchronous Machine", in Proc. ICEM 2000, August 2000, Espoo Finland, pp. 1251-1255.

Lee, J. H. and Hong, J. P. 2008. "Permanent magnet demagnetization characteristic analysis of a variable flux memory motor using coupled Preisach modeling and FEM," IEEE Trans. Magn., vol. 44, no. 6, pp. 1550-1553, Jun. 2008.

Lee, B.-K., Kang, G.-H., Hur, J., and You, D.-W. 2004. "Design of spoke type BLDC motors with high power density for traction applications," in Conf. Rec. 2004 IEEE Ind. Applicat. Conf. 39th IAS Annu. Meeting, Seattle, WA, 2004, vol. 2, pp. 1068-1074.

Lombard, P. 2009. Support Team Leader, CEDRAT S.A., France. Personal communication. patrick.lombard@cedrat.com, www.cedrat.com.

Markovic, M., Perriard, Y. 2007. "An analytical determination of eddycurrent losses in a configuration with a rotating permanent magnet," IEEE Trans. Magn., vol. 43, no. 8, pp. 3380-3386, Aug. 2007.

Markovic, M., Perriard, Y. 2008. "Analytical Solution for Rotor Eddy-Current Losses in a Slotless Permanent-Magnet Motor: The Case of Current Sheet Excitation", IEEE Trans. Magn., vol. 44, No. 3, pp. 386-393, March 2008.

Martinek, G. and Kronmüller, H. 1990. "Influence of grain orientation on the coercive field in Fe–Nd–B permanent magnets," J. Magn. Magn. Mat., vol. 86, pp. 177-183.

McCaig, M., Glegg, A.G. 1987. "Permanent magnets in theory and in practice", Pentech Press, London, Second Edition.

Mellor, P.H., Roberts, D., Turner, D.R. 1991. "Lumped parameter thermal model for electrical machines of TEFC design", IEE Proceedings B – Electric Power Applications, vol. 138, Issue: 5, Sep 1991, pp: 205 – 218, ISSN: 0143-7038.

Morimoto, S., Takeda, Y., Hirasa, T., Taniguchi, K. 1990. "Expansion of Operating Limits for Permanent Magnet Motor by Current Vector Control Considering Inverter Capacity", IEEE Transactions on Industry Applications, vol. 26, No. 5, pp. 866-871, September/October 1990.

Negrea, M., Arkkio, A., Jokinen, T., Hakuli, M. 2001. "Thermal analysis of a permanent magnet synchronous motor", Proceedings of the 2001 International Symposium on Diagnostics for Electrical Machines, Power Electronics and Drives, Grado, Italy, September 2001, pp: 517-522.

Negrea, M., Rosu, M. 2001. "Thermal analysis of a large permanent magnet synchronous motor for different permanent magnet rotor configurations", Electric Machines and Drives Conference, IEMDC 2001, pp: 777-781, ISBN: 0-7803-7091-0.

Neorem Magnets Oy, 2010. Web pages, [Online]. Available: http://www.neorem.fi.

Odor, F., Mohr, A. 1977. "Two-component magnets for DC motors", IEEE Trans. Magn., vol. MAG-13, No. 5, pp. 1161-1162, September 1977.

Odor, F., Mohr, A., Bolenz, K., Robert Bosch GmbH 1975. "Magnetic structure, particularly permanent magnet for motor fields, and method", United States Patent, Appl. No.: 618574, Filed: Oct. 1, 1975.

Ooshima, M., Miyazawa, S., Chiba, A., Nakamura, F., Fukao, T. 1997. "A Rotor Design of a Permanent Magnet-Type Bearingless Motor Considering Demagnetization", Power Conversion Conference, Nagaoka, August 1997, vol. 2, pp. 655-660.

Outokumpu Magnets Oy, 1990. Technical Manual, Pori, Finland.

Perez, I.J. and Kassakian, J. G. 1978. "Computer-Aided Design of High Speed Synchronous Machines", IEEE PES Summer Meeting, paper A 78 581-1.

Perez, I.J. and Kassakian, J. G. 1979. "A stationary thermal model for smooth air-gap rotating electric machines", Electric Machines and Electromechanics, No. 3-4, pp. 285-303.

Perho, J. 2002. "Reluctance network for analyzing induction machines", Diss., Helsinki University of Technology, Acta polytechnica Scandinavica, Electrical Engineering Series No. 110, Espoo, Finland.

Phelps, B., Atherton, D. 2001. "Pinning and minor Loops in an Inclusive Model of Ferromagnetic Hysteresis", IEEE Trans. Magn., vol. 37, No. 1, pp 517-521, Jan 2001.

Polinder, H., Hoeijmakers, M. J. 1997. "Eddy-current losses in the permanent magnets of a PM machine," in IEE Conf. EMD97, no. 444, pp. 138-142.

Polinder, H., Hoeijmakers, M. J. 1999. "Eddy-current losses in the segmented surface-mounted magnets of a PM machine," in IEE Proc.- Electr. Power Appl., vol. 146, no. 3, pp. 261-266, May 1999.

Rilla, M. 2006. "Kestomagneettitahtikoneen lämpömallinnus", Masters Thesis, Lappeenranta University of Technology, 23 (345), August 2006.

Rilla, M., Pyrhönen, J., Niemelä, M., Pekola, J., Jäppinen, J. 2008. "Design of a 60 kW, 9000 rpm non-salient pole Pm machine", in Proc. ICEM 2008, Paper ID 921, 4 pages.

Rodewald, W., Blank, R., Wall, B., Reppel, G.W., Zilg, H.D. 2000. "Production of Sintered Nd-Fe-B Magnets with a Maximum Energy Density of 53 MGOe", Proceedings of the Sixteenth International Workshop on Rare-Earth Magnets and Their Applications, Senda, Japan, September 2000, pp.: 119-126.

Rosero, J., Cusido, J., Garcia, A., Ortega, J., Romeral, L. 2006. "Study on the Permanent Magnet Demagnetization Fault in Permanent Magnet Synchronous Machines", IEEE Industrial Electronics, IECON 2006 - 32nd Annual Conference on, 6-10 Nov. 2006, pp: 879-884, ISBN: 1-4244-0390-1.

Rosero, J. Romeral, L. Ortega, J.A. Urresty, J.C. 2008. "Demagnetization fault detection by means of Hilbert Huang transform of the stator current decomposition in PMSM", IEEE International Symposium on Industrial Electronics, ISIE 2008, June 2008, pp: 172-177, ISBN: 978-1-4244-1665-3.

Rosu, M., Arkkio, A., Jokinen, T., Mantere, J., Westerlund, J. 1999. "Demagnetisation State Of Permanent Magnets In Large Output Power Permanent Magnet Synchronous Motor", Electric Machines and Drives, 1999, in Proc. International Conference IEMD '99, May 1999, Seattle, USA, pp. 776-778.

Rosu, M., Jokinen, T., Demeter, E. 1998. "Simulation of the Magnetic Hysteresis in NdFeB Permanent Magnet Using Preisach's Model", OPTIM'98, Optimization of Electrical and Electronic Equipments, Brasow, Romania, 11-14 May, 1998, p. 11-14.

Rosu, M., Saitz, J., and Arkkio, A. 2005. "Hysteresis model for finite-element analysis of permanent-magnet demagnetization in a large synchronous motor under a fault condition," IEEE Trans. Magn., vol. 41, no. 6, pp. 2118-2123, June 2005.

Russell, R. L.; Norsworthy, K. H. 1958. "Eddy current and wall losses in screened-rotor induction motors", Proc. of IEE, p.163-175, April 1958.

Saari, J. 1995. "Thermal modeling of high-speed induction machines", Licenciate Thesis, Helsinki University of Finland, Acta Polytechnica Scandinavica, Electrical Engineering Series No. 82, Helsinki, Finland, ISBN: 951-666-454-7.

Saari, J. 1998. "Thermal Analysis of High-speed Induction Machines", Diss., Acta Polytechnica Scandinavica, Electrical Engineering Series No. 90, Helsinki, Finland.

Sagawa, M.2007. INTERMETALLICS Co., Ltd, Japan. Personal communication, May 2007. sagawa@intermetallics.co.jp, www.intermetallics.co.jp

Schmidt, K., Sterz, O., Hiptmair, R. 2009. "Estimating the Eddy-Current Modeling Error", IEEE Trans. Magn., vol. 44, no. 6, pp. 686-689, June 2009.

Skomski, R., Coey, J. M. D. 1999. "Permanent Magnetism", Institute of Physics Publishing Ltd, ISBN 07503 0478 2, pp 191-204.

Thelin, P. 2002. "Short circuit fault conditions of a buried PMSM investigated with FEM", Proceedings of the Nordic Workshop on Power and Industrial Electronics, NORpie, August 2002.

Thuillier, T., Curdy, J.-C., Lamy, T., Sole, P., Sortais, P., Vieux-Rochaz, J.-L., Voulot, D. 2004. "Advanced magnetic calculations for high magnetic field compact ion source", Review of scientific instruments, vol. 75 (2), no. 5, pp. 1526-1528.

Toda, H., Xia, Z., Wang, J., Atallah, K., Howe, D. 2004, "Rotor Eddy-Current Loss in Permanent Magnet Brushless Machines", IEEE Trans. Magn., vol. 40, no. 4, pp. 2104-2106, July 2004.

Trout, S. 2001, "Material Selection of Permanent Magnets, Considering Thermal Properties Correctly", Electric Manufacturing and Coil Winding Conference, Cincinnati, Ohio, USA, October 2001, 6 pages.

Vacuumschmelze, 2008. PD 002-VACODYM/VACOMAX, EDITION 2007 S. The Brochyre Permanent Magnets, [Online]. Available: http://www.vacuumschmelze.de/dynamic/docroot/medialib/documents/broschueren/dm brosch/PD-002_e_310807.pdf, pp. 14-17, 07.02.2008.

Wang, J., Wang, W., Atallah, K. and Howe, D. 2008, "Demagnetization assessment for three-phase tubular brushless permanent-magnet machines", IEEE Trans. Magn., vol. 44, no. 9, pp. 2195-2203, Sep. 2008.

Wohlfarth, E. P. 1984. "The coefficient of magnetic viscosity", J. Phys. F: Metal Phys., vol. 14, p. L155.

Wu, K., Yao, Y., Klik, I., 1997. "Electrical and magnetic properties of NdFeB films," Appl. Surf. Sci., pp. 174-177.

Wu, W., Dunlop, J., Collocott, S. 2002. "Modelling of Eddy-Current Losses in a Surface-Mounted NdFeB Permanent-Magnet Generator", International Workshop on Rare-Earth Magnets and Applications, REPM2002, Newark, USA, August 2002, Proceedings, pp. 323-328.

Xi, X., Changming, C., Meng, Z. 2008. "Magnet demagnetization observation of permanent magnet synchronous motor", International Conference on Electrical Machines and Systems, ICEMS 2008, Oct. 2008, pp: 3216-3219, ISBN: 978-1-4244-3826-6.

Yao, Y., Jen, S., Chen, W., Horng, J., Wu, M., Anderson, E. 1988. "Electrical resistivity and magnetization studies of the NdFeB system," Chin. J. Phys., vol. 26, no. 4.

Zhu, Z., Ng, K., Howe, D. 2004. "Improved analytical modeling of rotor eddy current loss in brushless machines equipped with surface-mounted magnets", Proc. Inst. Elect. Eng., Elect. Power Appl., vol. 151, no. 6, pp. 641-650.

The permanent magnet electric machines are designed to remain fully magnetized in all working conditions. Still, the permanent magnets in a machine can lose a part of their magnetic strength, or demagnetize, if they are overheated or overloaded. In these cases it is important to be able to calculate the properties of a machine after irreversible demagnetization.

A tool able to simulate the behavior of a permanent magnet machine after demagnetization is developed. The tool includes a demagnetization model, an eddy current model, and a thermal model. The demagnetization model is validated by modeling a locked-rotor situation of a permanent magnet machine. The results are compared with the measured demagnetization of the magnets after the same situation. It is also studied, how the demagnetization should be modeled in different situations.

The eddy current calculation accuracy is improved by introducing the resistivity of NdFeB permanent magnet material as a function of temperature.

BUSINESS +
ECONOMY

ART +
DESIGN +
ARCHITECTURE

SCIENCE +
TECHNOLOGY

CROSSOVER

DOCTORAL
DISSERTATIONS